

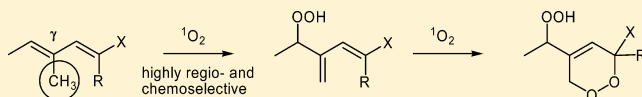
Ene–Diene Transmissive Cycloaddition Reactions with Singlet Oxygen: The Vinylogous Gem Effect and Its Use for Polyoxyfunctionalization of Dienes

Angelika Eske, Bernd Goldfuss, Axel G. Griesbeck,* Alan de Kiff, Margarethe Kleczka, Matthias Leven, Jörg-M. Neudörfel, and Moritz Vollmer

Department of Chemistry, University of Cologne, Greinstr. 4, D-50939 Cologne, Germany

Supporting Information

ABSTRACT: The singlet oxygen reactivities and regioselectivities of the model compounds **1b–d** were compared with those of the geminal (gem) selectivity model ethyl tiglate (**1a**). The kinetic cis effect is $k_E/k_Z = 5.2$ for the tiglate/angelate system **1a/1a'** without a change in the high gem regioselectivity. Further conjugation to vinyl groups enabled mode-selective processes, namely, $[4 + 2]$ cycloadditions versus ene reactions. The site-specific effects of methylation on the mode selectivity and the regioselectivity of the ene reaction were studied for dienes **1e–g**. A vinylogous gem effect was observed for the γ,δ -dimethylated and α,γ,δ -trimethylated substrates **1h** and **1i**, respectively. The corresponding phenylated substrates **1j–l** showed similar mode selectivity, as monomethylated **1j** exhibited exclusively $[4 + 2]$ reactivity while the tandem products **12** and **14** were isolated from the di- and trimethylated substrates **1k** and **1l**, respectively. The vinylogous gem effect favors the formation of 1,3-dienes from the substrates, and thus, secondary singlet oxygen addition was observed to give hydroperoxy-1,2-dioxenes **19** and **20** in an ene–diene transmissive cycloaddition sequence. These products were reduced to give alcohols (**16**, **17**, and **18**) or furans (**24** and **25**), respectively, or treated with titanium(IV) alkoxides to give the epoxy alcohols **26** and **27**. The vinylogous gem effect is rationalized by DFT calculations showing that biradicals are the low-energy intermediates and that no reaction path bifurcations compete.



INTRODUCTION

The singlet oxygen ene reaction is one of the synthetically most versatile photooxygenation protocols.¹ Not only are allylic hydroperoxides (the initial products of the Schenck ene reaction with $^1\text{O}_2$) available by this process, but also, allylic alcohols, epoxides, epoxy alcohols, 1,2-diols, and 1,2,3-triols can be obtained via simple reductive or transition-metal-catalyzed transformations.² Several mechanistic scenarios have been postulated for this reaction because numerous characteristics of this process are not in agreement with a symmetry-allowed concerted reaction course.³ Classical two-step processes involving 1,4-biradical, 1,4-zwitterion, perepoxide, dioxetane, or exciplex intermediates have been discussed.⁴ The results of inter- and intramolecular isotope experiments with isotopically labeled tetramethylethylenes provided evidence for suprafacial $^1\text{O}_2$ attack and for a perepoxide intermediate.⁵ Also, the small negative activation enthalpies and highly negative activation entropies observed for the singlet oxygen ene reaction argue for the participation of a reversibly formed exciplex as an intermediate.⁶ Recently, the two-step no-intermediate mechanism involving a bifurcating transition state with a perepoxide structure was proposed by Houk and co-workers.⁷ Small changes in the substrate structure can also open a low-energy pathway via a real perepoxide intermediate.⁸ The valley ridge model⁹ appears to be a powerful explanation of the cis effect (vide infra) as well as deviations that result from geometrical constraints of the allylic hydrogen atoms.¹⁰

For 1,3-dienes or higher polyenes, additional chemical and physical processes can compete with the ene process, including $[2 + 2]$ and $[4 + 2]$ cycloadditions and physical quenching of singlet oxygen.¹¹ The latter process often dominates with extended polyenes such as several carotenoids or tocopherols that quench singlet oxygen with near-diffusion-controlled rates.¹² Under cellular conditions, however, this protective behavior was recently questioned for β -carotene.¹³ Other carotenoids and apocarotenoids show competing physical and chemical quenching of singlet oxygen.¹⁴ Among these dienes, crocin (Figure 1) represents an α,ω -dimethylated tetradecaheptaene-1,14-dicarboxylic acid that has been found to

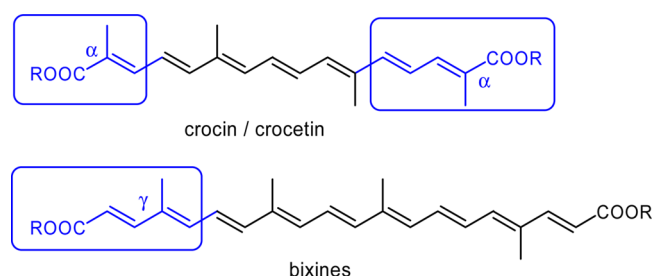


Figure 1. Apocarotenoids with relevant structure motifs.

Received: January 23, 2014

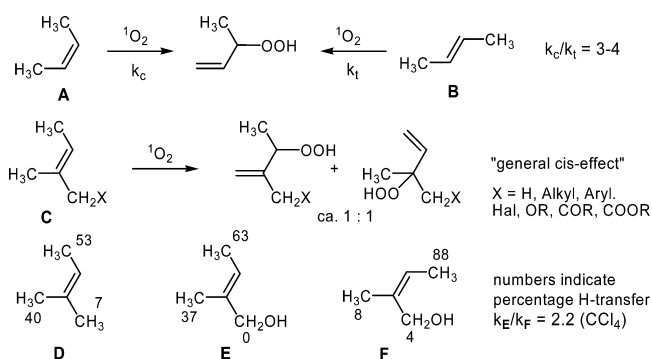
Published: January 29, 2014

chemically react with singlet oxygen with a rate constant of $0.56 \times 10^8 \text{ M}^{-1} \text{ s}^{-1}$ in water.¹⁵ The corresponding bixines (Figure 1) are γ -methylated octadecanonaenes with similar singlet oxygen reactivity. Obviously, these compounds have multiple sites for singlet oxygen reactions, and diverse primary and secondary processes can be expected. However, no detailed studies of the primary chemical reaction events or the structures of the first peroxidic products with these apocarotenoids have been reported. In an initial approach to this problem, we identified three critical substrate motifs in these biological substrates: (a) the tiglate-type structure with the potential ene-reactive α -methyl group, (b) the α -methylated diene ester, and (c) the γ -methylated diene ester motifs. This study aimed to investigate the (chemical) singlet oxygen reactivity with these structural motifs in order to determine the influence of β -vinylation of the methacrylate system in type (a) and the introduction of methyl groups at the α -, γ -, and δ -positions of enone esters as exist in types (b) and (c).

RESULTS

Cis and Gem Effects with Monoalkenes and Michael Esters. The term *cis effect* describes a kinetic preference of alkenes with two reactive groups at positions 1 and 2 in the *cis* configuration in comparison with the corresponding *trans* isomer. For singlet oxygen ene reactions, this definition is often extended and also includes the *regioselectivity* of the hydrogen transfer, meaning that CH activation is preferred for alkene sites with the *cis* configuration of groups presenting allylic hydrogens. This phenomenon, which was investigated in-depth by extensive substrate variation and sophisticated kinetic isotope and product isotope effects, has been interpreted as a hint for the perepoxide intermediate model. Following this model, in the rate-determining step of the singlet oxygen ene reaction, a twofold interaction between $^1\text{O}_2$ and the allylic hydrogens accelerates the reaction by a factor of 3–4 for *cis*-2-butene (A) versus *trans*-2-butene (B) (Scheme 1).¹⁶ This

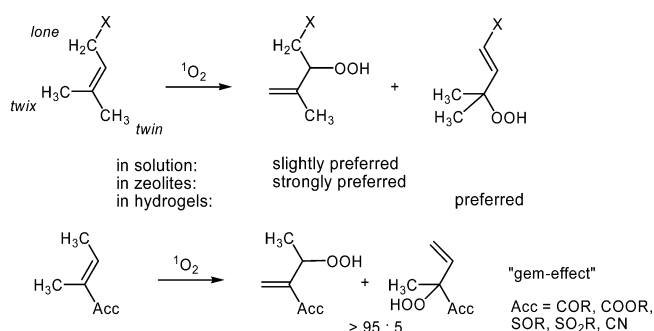
Scheme 1. Regioselectivity Trends in Singlet Oxygen Ene Reactions: Cis Effect



primary interaction is also represented in the regioisomer ratios. For example, for 2-methyl-2-butene (D), hydrogen transfer from the higher-substituted site of the alkene prevails by 93%. Two methyl groups in the *cis* configuration (C) give optimal *cis* effects with respect to the total reactivity and regioselectivity. The third (*twin*) methyl in D contributes only 7% of the hydrogen transfer.¹⁷ For the diastereomeric allylic alcohols E and F, the *product cis* effects are 100% for E and 92% for F,¹⁸ while the *kinetic cis* effect (k_E/k_F) is 2.2 for these substrates.

The locants *lone*, *twix*, and *twin* are also used to describe the regions in trisubstituted alkenes (Scheme 2). For the *cis* effect,

Scheme 2. Regioselectivity Trends in Singlet Oxygen Ene Reactions: Medium and Gem Effects

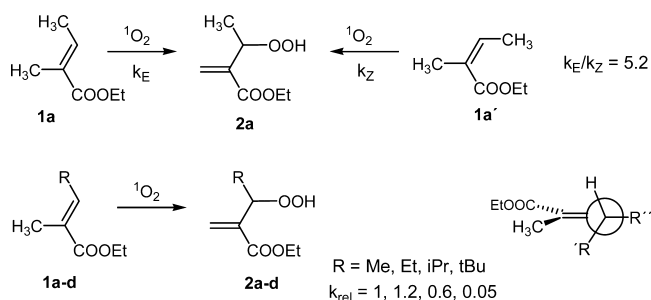


preferential hydrogen interaction and subsequent abstraction from the *lone* and *twin* positions is observed in solution. This effect is nearly independent of the nature of the allylic substituent X. Under restricted environment conditions, however, this selectivity is altered: in zeolites, the *twix* selectivity dominates strongly,¹⁹ whereas in microemulsions and more noticeably in hydrogels, hydrogen abstraction from the *lone* methylene group becomes prevalent.²⁰ Another very strong regiodirecting effect was observed for acceptor-substituted 2-butenes. This phenomenon, termed the *gem effect*, describes the regioselective ene reaction of $^1\text{O}_2$ with α,β -unsaturated carbonyl compounds and carbonyl analogues (nitriles, sulfoxides, and sulfonates).²¹ There is only a little environmental influence on this kind of selectivity effect.²²

Tiglate Substrates and 1,3-Diene-1-carboxylates: Reactivity and Selectivity Studies.

In order to evaluate the kinetic contribution of the *cis* effect, we compared the reactivities of the *E* and *Z* isomers of 2-methyl-2-butenic acid ethyl ester (1a and 1a', respectively). Both stereoisomers result in the *gem*-type allylic hydroperoxide 2a with diastereoselectivities of >98% (Scheme 3), that is, there exists no *cis* effect in the

Scheme 3. Singlet Oxygen Ene Reactions with Tiglate and Angelate Esters and Their Derivatives



product-forming step. The kinetic *cis* effect was determined from the pseudo-first-order substrate consumption curves depicted in Figure 2 (a 1:1 mixture of alkene double-bond isomers was reacted with $^1\text{O}_2$ in CCl_4). In agreement with the oxygen uptake curves, the curve progression switch to second-order behavior after 70% conversion and a kinetic *cis* effect of 5.2 were determined for 1a and 1a'. A subsequent decrease in the kinetic *cis* effect is expected for a decreasing number of allylic hydrogens on the β -alkyl group. The β -ethyl substrate 1b

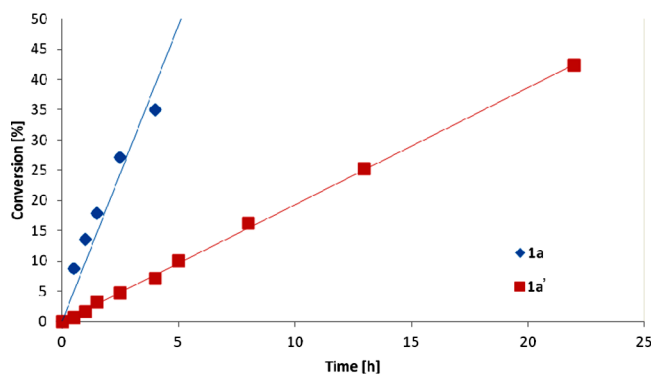


Figure 2. Singlet oxygen ene reaction with ethyl tiglate (**1a**) vs ethyl angelate (**1a'**).

($R' = H$, $R'' = Me$) reacted slightly faster with 1O_2 , possibly because 1,3-allylic strain positions the allylic hydrogens in the optimal perpendicular orientation on both sides of the π -system. This effect breaks down for one side of the π -system for the β -isopropyl substrate **1c** ($R' = R'' = Me$) and completely for the *tert*-butyl substrate **1d**, resulting in a relative kinetic situation of 1:1.2:0.6:0.05 for **1a**:**1b**:**1c**:**1d** (Figure 3).

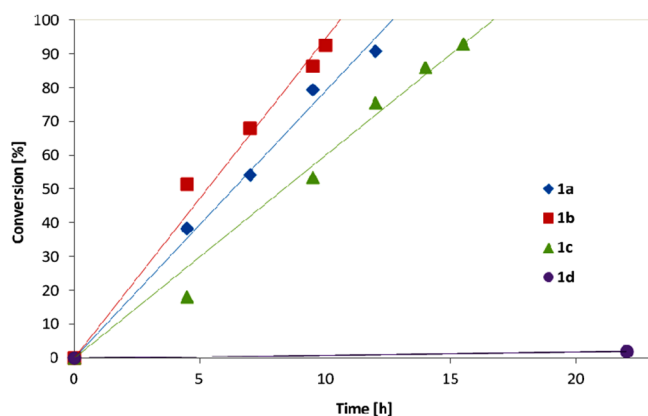
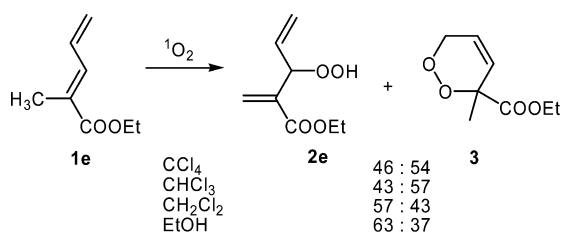


Figure 3. Singlet oxygen ene reaction with β -alkylated *E*-configured substrates **1a–d**.

A substantial electronic modification of the tiglate system results from the incorporation of the β -vinyl group in **1e**. This compound shows solvent-dependent mode selectivity between the $[4 + 2]$ cycloaddition and the ene reaction with 1O_2 (Scheme 4). The ene reaction, which is suspected to proceed via a more polar transition state compared with the asynchronous $[4 + 2]$ process,²³ became the dominant process in polar protic solvents. The kinetic comparison with substrate **1b** exhibiting the maximum kinetic cis effect (see Figure 2)

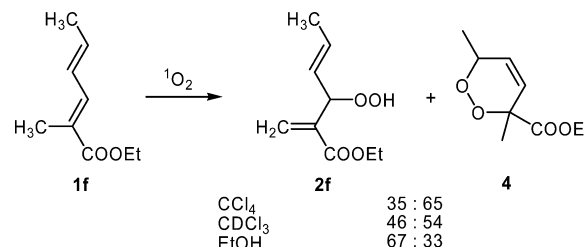
Scheme 4. Solvent Dependence of the Singlet Oxygen Ene Reaction with **1e**



shows a rate decrease by a factor of 40 for the ene reaction with **1e**. Overall, the mode selectivity (i.e., ene vs $[4 + 2]$ reaction mode) is low for this substrate with no ene regio differentiation possible here.

A comparable solvent effect on the mode selectivity was observed for the α,δ -dimethylated substrate **1f** (Scheme 5). The

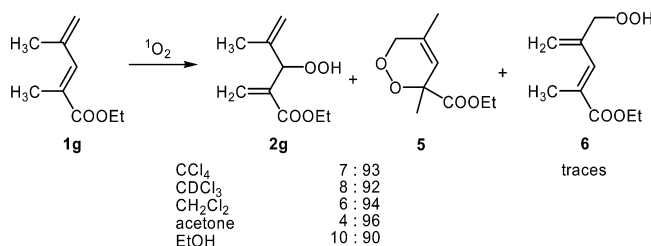
Scheme 5. Solvent Dependence of the Singlet Oxygen Ene Reaction with **1f**



δ -methyl group was completely inert under the reaction conditions even after prolonged irradiation time, and the ene product **2f** from α -hydrogen transfer was dominant in ethanol, where the reaction could only be processed to 52% conversion. The additional methyl group in **1f** accelerates the singlet oxygen reaction by a factor of 5 in comparison with **1e**.

The picture changed substantially for the α,γ -dimethylated substrate **1g** (Scheme 6). The solvent effect on the mode

Scheme 6. Solvent Dependence of the Singlet Oxygen Ene Reaction with **1g**



selectivity vanished nearly completely, and under all solvent conditions endoperoxide **5** was obtained as the major product with complete conversion in nonpolar solvents after less than 24 h. Compound **5** was crystallized from acetone and characterized by X-ray structure analysis (Figure 4).²⁴ Upon comparison of the reactivities of the two methyl groups at the α - and γ -positions, the α -hydrogen transfer product **2g** was observed and isolated as the respective allylic alcohol, whereas

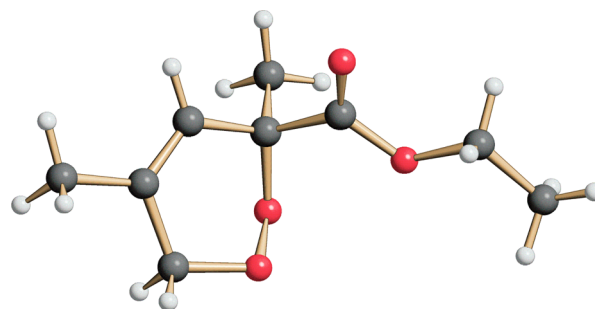
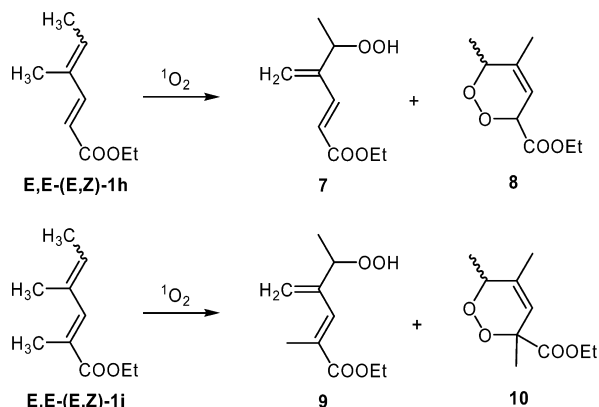


Figure 4. Crystal structure of endoperoxide **5**.

less than a 2% yield of the γ -hydrogen transfer product **6** was observed by ^1H NMR analysis.

The next diene substrate, γ,δ -dimethylated **1h**, was investigated as the pure *E,E* diastereoisomer as well as a 9:1 mixture of the *E,Z* and *E,E* diastereoisomers (Scheme 7). In

Scheme 7. Singlet Oxygen Ene Reactions with *E,E*(*E,Z*)-1h** and *E,E*(*E,Z*)-**1i****



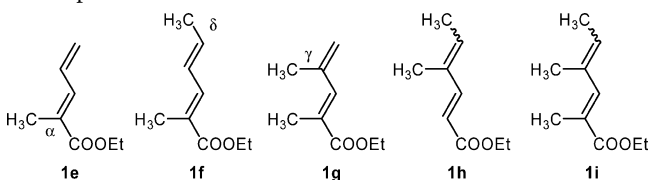
both cases, rapid singlet oxygen addition delivered the allylic hydroperoxide **7** as the sole product after >90% conversion of the starting material. Even faster were the reactions of singlet oxygen with the α,γ,δ -trimethylated substrates **1i** (also applied as the pure *E,E* diastereoisomer as well as a 4:1 mixture of the *E,Z* and *E,E* isomers), which delivered allylic hydroperoxide **9**. In both cases, only trace amounts of the corresponding [4 + 2] cycloadducts **8** and **10**, respectively, were observed in the NMR spectra. Upon further treatment of the substrate solutions with singlet oxygen, the tandem products **19** and **20** were formed (see later).

The most reactive substrate in this series of 1,3-diene carboxylates is the *E,E* isomer of **1i** (Table 1). Obviously, this substrate profits from the kinetic cis effect as well as from the highly nucleophilic diene structure. Remarkably, substrate **1i**

Table 1. Singlet Oxygen Ene Reactions with 1,3-Diene Carboxylates **1e–i in CDCl_3**

substrate	Me subst. pattern	$t_{>90\%}$ (h) ^a	k_{rel} ^b	yields (%)		
				α -ene	γ -ene	[4 + 2]
1e	α	120	5	56	—	44
1f	α,δ	48	16	35	—	65
1g	α,γ	22	30	6	1	93
<i>E,E</i> - 1h	γ,δ	12	50 ^c	—	>98	<2
<i>E,Z</i> - 1h	γ,δ	28	23 ^{c,d}	—	>98	<2
<i>E,E</i> - 1i	α,γ,δ	6	100 ^e	—	>98	<2
<i>E,Z</i> - 1i	α,γ,δ	13	48 ^{d,e}	—	>98	<2

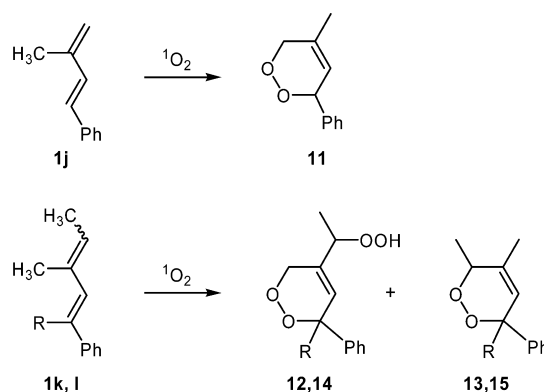
^aTime needed for >90% conversion as determined by ^1H NMR analysis. ^bThe value for the fastest substrate, *E,E*-**1i**, was set to 100. ^cCorresponds to a kinetic cis effect of 2.2. ^dCorrected to 100% *E,Z*. ^eCorresponds to a kinetic cis effect of 2.1.



has the largest number of reaction possibilities, including three different methyl groups for ene reactions as well as the 1,3-diene moiety for [4 + 2] cycloaddition. Conformational reasons cannot be responsible for the prevalence of the ene process because no substantial difference in the *s*-cis/*s*-trans conformational ratio can be expected for **1g** in comparison with *E,E*-**1i**. Thus, this scenario of mode and ene regioselectivity is a perfect example for a kinetic Curtin–Hammett situation. The computational aspects of the strong vinylogous gem selectivities of **1h** and **1i** are discussed later.

1-Phenyl-1,3-dienes: Reactivity and Selectivity Studies. In order to evaluate the effect of conjugation preservation (vide infra) as the decisive factor for regiocontrol in the gem and vinylogous gem effects, substrates **1j–l** with a phenyl group instead of the carboxy group in **1a–i** were studied. In the absence of a kinetic cis effect, diene **1j** prefers [4 + 2] reactivity in a slow singlet oxygen reaction (Scheme 8).

Scheme 8. Singlet Oxygen Ene Reactions with **1j, *E,Z*-**1k**, and *E,Z*-**1l****



The di- and trimethylated substrates **1k** and **1l**, however, showed high vinylogous gem regioselectivity. The analogy to the ester substrates **1h** and **1i** is apparent. A moderately higher singlet oxygen reactivity and a decreased mode selectivity (i.e., more [4 + 2] cycloaddition products **13** and **15**) were observed in the crude reaction mixture from the phenylated substrates **1k** and **1l** (Table 2). However, no primary ene adducts could be

Table 2. Singlet Oxygen Ene Reactions with 1-Phenyl-1,3-dienes **1j–l in CDCl_3**

substrate	Me subst. pattern	$t_{>90\%}$ (h) ^a	yields (%)		
			α -ene	γ -ene	[4 + 2]
1j	γ	48	—	<5	>95
1k	γ,δ (R = H)	24	—	93 ^b	7 (13)
1l	α,γ,δ (R = Me)	10	<2	73 ^b	27 (15)

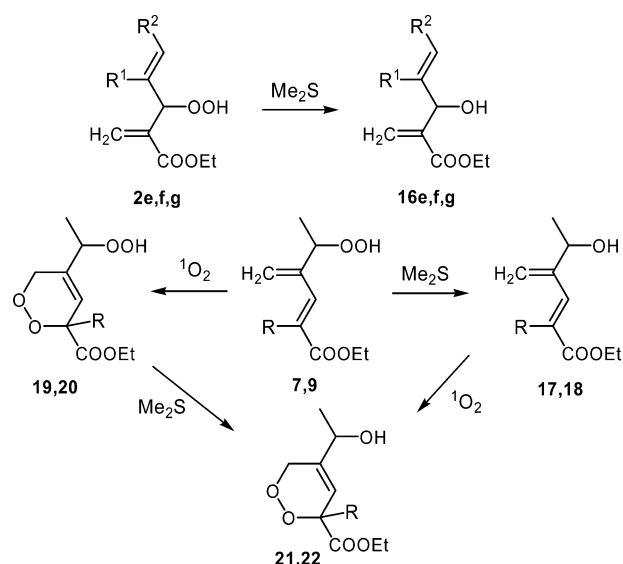
^aTime for >90% conversion as determined by ^1H NMR analysis.

^bBased on tandem products (**12** from **1k** and **14** from **1l**) from a sequence of γ -ene followed by [4 + 2] cycloaddition.

observed from these substrates because the secondary singlet oxygen [4 + 2] cycloadditions were faster than the primary ene processes, so only the tandem products **12** and **14**, respectively, were isolated. The reaction times indicated in Table 2 thus describe the quantitative addition of two singlet oxygen molecules in a consecutive way for the substrates **1k** and **1l**.

Further Tandem and Oxyfunctionalization Reactions. In most cases, the dienyl hydroperoxides from gem- or

Scheme 9. Reduction of Ene Products and Tandem Processes with 1,3-Dienes **7** and **9**



vinyllogous-gem-selective ene reactions were not stable under standard purification procedures. In these instances, reduction to the stable diene carbinols was performed with dimethyl sulfide, and these compounds were investigated as substrates

for further singlet oxygenation (i.e., in tandem singlet oxygen with combined reduction). Whereas the allylic alcohols **16e–g** were nonreactive, the diene hydroperoxides **7** and **9** did add a second singlet oxygen molecule to give the 1,2-dioxenes **19** and **20**, respectively, as did the diene carbinols **17** and **18** to give **21** and **22**, respectively (Scheme 9).²⁵ In Figure 5, three NMR traces are shown that demonstrate the cleanness of these tandem processes: photooxygenation of diene **1i** and subsequent reduction with dimethyl sulfide delivered diene alcohol **18** after a short irradiation time. The subsequent slower photooxygenation delivered endoperoxide **22** as a mixture of diastereoisomers. In the case of the arylated substrates **1k** and **1l**, this rate difference was inverted, and thus, only the tandem products **12** and **14**, respectively, were obtained (vide supra).

The tandem process could likewise be performed without isolation of the intermediate hydroperoxides by prolonged irradiation of the sensitizer-containing reaction mixture, leading to bisperoxides **19** and **20**, respectively. Reduction of these products with dimethyl sulfide gave the identical products as the three-step oxygenation/reduction/oxygenation route in comparable overall yields (Scheme 9).

The reduction of 1,2-dioxenes with thiourea resulted in the corresponding furans (Scheme 10).²⁶ The tandem product **12** (from **1k**) was reduced to hydroxy 1,2-dioxene **23** and subsequently converted to furan **24**, and accordingly, this reaction sequence delivered furan **23** from substrate **1h** via tandem singlet oxygenation and one-pot reduction with

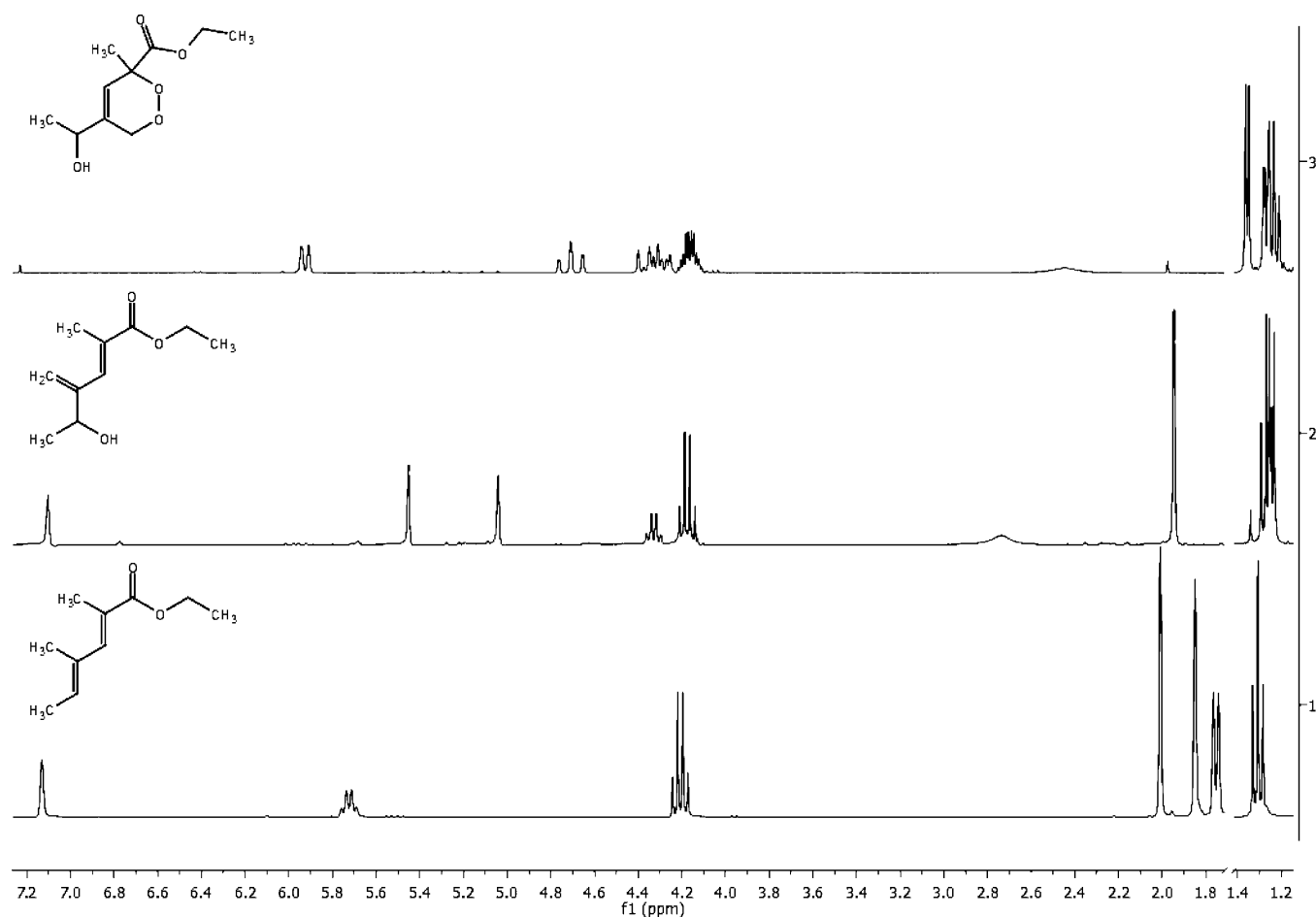
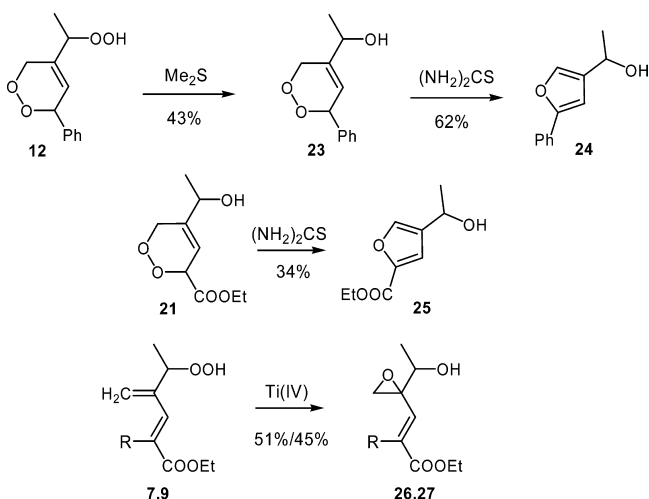


Figure 5. ¹H NMR spectra of (1) diene **E,E-1i**, (2) dienol **18** (after 6 h of reaction time and reduction), and (3) tandem product **22** (diastereoisomeric mixture, 1:1).

Scheme 10. Secondary Transformations of 1,2-Dioxenes and Allylic Hydroperoxides



dimethyl sulfide and thiourea. Another useful transformation of allylic hydroperoxides was also applied in this investigation, namely, titanium(IV)-catalyzed oxygen transfer to give epoxy alcohols.²⁷ The primary singlet oxygen addition products with the diene esters **1h** and **1i** (the allylic hydroperoxides **7** and **9**, respectively) were transformed in situ into the epoxy alcohols **26** and **27**, respectively, by treatment of the crude reaction mixture (after uptake of 1 equiv of oxygen) with catalytic amounts of titanium tetraisopropoxide. Thus, the tandem products as well as the primary addition products are useful substrates for further oxyfunctionalization.

Vinylogous Gem Effect: Theoretical Studies. The reactions of dienes **E,E-1h** and **E,Z-1h** with singlet oxygen were also investigated computationally by means of density functional theory in order to rationalize the *high vinylogous gem regioselectivity* that favors the formation of the conjugated

product **7** (Figure 6). Both possible pathways (to **7** and **7'**) were calculated for each substrate employing the nonempirical TPSS functional developed by Staroverov et al.²⁸ to reach high accuracy for the description of hydrogen abstraction. All of the computations were carried out as unrestricted DFT to allow spin contamination within the ground-state determinant description of biradical intermediates and the TZVP basis set from Ahlrich et al.²⁹ was used.

It was theoretically evaluated by Maranzana et al. in 2005 that α,β -unsaturated carbonyl compounds are prone to form biradical intermediates in Schenck ene-type reactions.³⁰ Similar reaction paths were also found for the substrates **E,E-1h** and **E,Z-1h**. The reaction coordinate depicted in Figure 6, corresponding to the transformation of **1h**, starts with the addition of singlet oxygen to generate the conjugated biradical intermediate **BR_a**. Alternatively, the nonconjugated biradical **BR_c** can be generated, from which eventually the regioisomeric product **7'** results. However, it was found that the nonconjugated intermediate **BR_c** is not a stationary point on the potential energy surface, so all further downstream products originate in **7**. The regioselectivity-determining hydrogen abstraction follows the initial biradical stage. As depicted in Figure 6, the activation barrier for the formation of the experimentally found product **7** is almost zero (0.3 kcal/mol). The formation of the disfavored product **7'** from the low-lying biradical intermediate is clearly kinetically hindered since the activation barrier for the corresponding hydrogen abstraction and 1,2-oxygen migration (nonleast motion) is 7.7 kcal/mol (**TS2_a**). On the thermodynamic side, comparison of the possible products **7** and **7'** does also show a clear preference for the experimentally favored product **7** as well. Product **7**, which exhibits a larger conjugated double bond system is energetically favored by 4.6 kcal/mol. The reaction coordinate for the ene reaction of the double-bond-isomeric diene **E,Z-1h** with singlet oxygen exhibits very similar properties. Again, there is only one minimum biradical intermediate, **BR_b**, which is

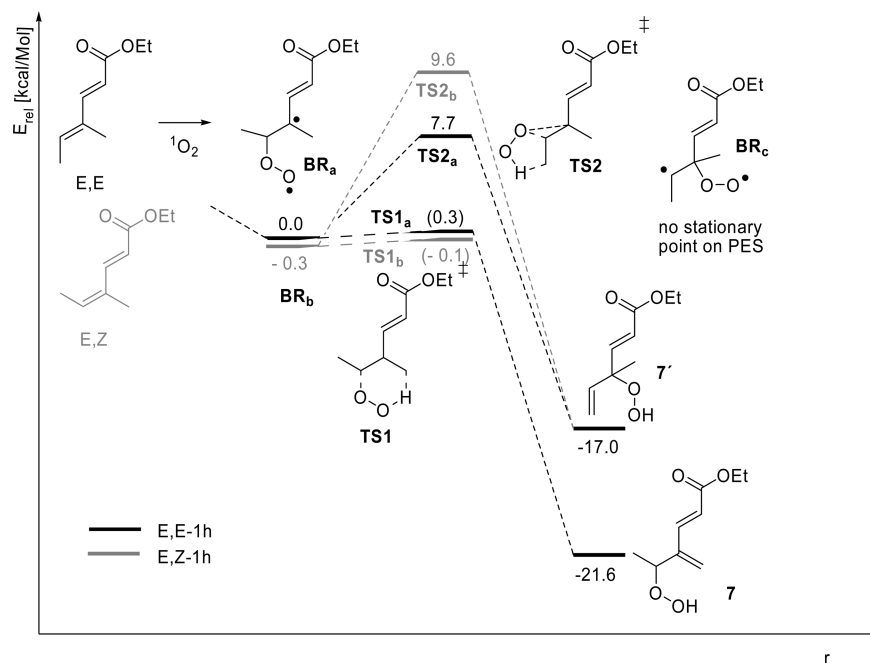


Figure 6. Computational analysis of the singlet oxygen ene reactions of **E,E-1h** and **E,Z-1h**. The experimentally determined regioselectivities originate in the almost barrierless pathways including transition states **TS1_a** and **TS1_b**, respectively.

slightly lower in energy than BR_a . There is also a very small activation barrier of 0.2 kcal/mol, via $TS1_b$, for the hydrogen abstraction that leads to the favored product 7, whereas the transition state $TS2_b$ leading to the disfavored product 7' is markedly higher in energy than $TS2_a$. The downstream structures derived from E,Z -1h differ from the intermediate BR_a and the transition states $TS1_a$ and $TS2_a$ only by slight conformational distortions that even increase the selectivity for the hydrogen abstraction for E,Z -1h (Figure 6). A conformational equilibrium at the biradical stage is most unlikely, since every rotation barrier will be much higher in energy than $TS1_a$ and $TS1_b$ and conformational equilibrium is eventually established at the product hydroperoxide stage.

A closer look at the competing transition structures in the regiodetermining step (Figure 7) elucidates why the favored

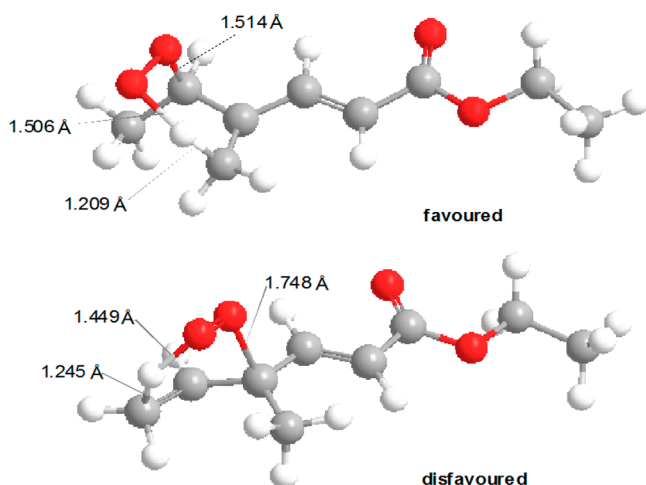


Figure 7. Competing transition structures for hydrogen abstraction, $TS1_a$ and $TS2_a$ (TPSS/TZVP).

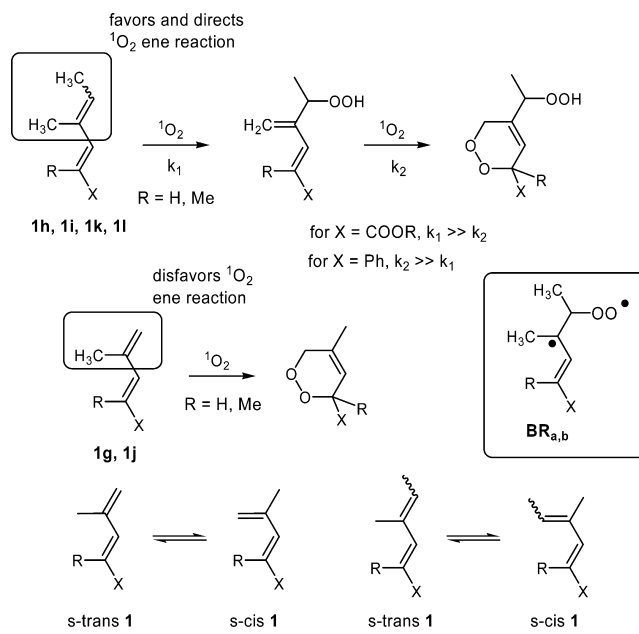
pathway exhibits a much lower activation barrier. The bond length between the peroxy group and the carbon framework in $TS1_a$ is 1.514 Å. The corresponding oxygen–carbon distance in the disfavored counterpart $TS2_a$ is markedly longer (1.748 Å). This difference is due to a synchronous 1,2-shift of the peroxy group that includes C–O bond cleavage. On the other hand, it is apparent that the conjugated double bond system is separated in the moment of the oxygen shift.

From the results of this study, a mechanistic rationale for the singlet oxygen reaction with 1,3-diene carboxylates and the corresponding 1-phenyl-1,3-dienes can be derived. The results for the singlet oxygen reactivities of the E/Z isomers $1a/1a'$ as well as the double-bond isomers of the ester- and phenyl-substituted dienes $1h,i$ and $1k,l$, respectively, indicate that the so-called cis effect leads to a kinetic preference for substrates with two methyl groups in the cis configuration without influencing the ene regioselectivity (Scheme 11). Irrespective of the double-bond configuration, all of the substrates resulted in high gem or vinylogous gem selectivity. Substrates bearing only one methyl group at C-3 preferentially gave [4 + 2] cycloaddition products (93% from **1g**, 100% from **1j**).

CONCLUSION

The apparently decisive factor for directing the mode selectivity (i.e., ene versus [4 + 2] reactivity) is the additional (and totally unreactive) methyl group at the terminal diene carbon, irrespective of whether it is in the Z or E configuration.

Scheme 11. Substituent Dependence of 1O_2 Addition to 1,3-Dienes; Biradical Intermediates $BR_{a,b}$ and the s -cis/ s -trans Conformational Situation for Mono- and Dimethylated Substrates



These effects and the theoretical calculations account for a two-step reaction mechanism. In the first step, via a perepoxide-like transition state, a biradical intermediate is formed that undergoes hydrogen abstraction from a geminal or vinylogous geminal position. If the first step is kinetically not favored, either by the missing terminal methyl group or by the nonexistent cis effect, the [4 + 2] cycloaddition reaction prevails, most likely proceeding as an asynchronous concerted cycloaddition.

Calculations showed that the regioselectivity of the singlet oxygen ene reactions with the di- and trimethylated substrates **1h–l** results from a biradical BR_a that is converted by a nearly barrier-free process to the corresponding hydrogen transfer product with vinylogous gem selectivity.

EXPERIMENTAL SECTION

General Aspects and Methods. *meso*-Tetraphenylporphyrin (TPP) was purchased from Porphyrin Systems (Bremen, Germany). The solvents for solution photooxygenation were puriss. and used as purchased. 1H and ^{13}C NMR spectra were recorded at 300, 500, or 600 MHz for 1H and 75.4, 125.7, or 150.9 MHz for ^{13}C . Chemical shifts are reported in parts per million relative to tetramethylsilane with the solvent resonances of $CDCl_3$ as the internal standards (center line of the triplet at 77.0 ppm for ^{13}C and the singlet at 7.24 ppm for 1H). Mass spectra and accurate mass determinations were obtained by direct-inlet electrospray ionization (EI). Infrared spectra were recorded with a Fourier transform (FT-IR) spectrometer. Samples were scanned as neat liquids or dissolved in CH_2Cl_2 . For all of the new compounds, satisfactory elemental analyses and high-resolution mass spectra as well as HPLC and/or GC analyses were obtained that confirmed >95% purity. For the photooxygenation reactions, either a halogen street lamp (150 W) or white LEDs were used.

Preparation of Compounds 1. General Procedure for Horner–Wittig Reactions (GP-A). To a suspension of *tert*-butoxide (2 equiv) in dry THF (2 mL per mmol of aldehyde) under argon was added slowly triethyl phosphonoacetate (1 equiv). After the mixture was stirred for 15 min, the aldehyde (1 equiv) was added dropwise to the solution. The mixture was allowed to stir for 2 h before the reaction was

quenched by the addition of water, after which the mixture was extracted three times with diethyl ether. The combined extracts were washed with brine and dried with MgSO_4 . The solvent was evaporated under reduced pressure, and the crude product was purified by column chromatography.

General Procedure for Wittig Reactions (GP-B). Freshly prepared 1-ethoxycarbonyl ethylidene triphenylphosphane (1 equiv) was reacted with the aldehyde (1 equiv) in toluene (1 mL per mmol of aldehyde) at 100 °C for 24 h. The solvent was removed under reduced pressure, and the crude product was dissolved in *n*-pentane, separated from the solid by filtration, and purified by column chromatography.

(E)-Ethyl 2-Methylpent-2-enoate (1b).³² The crude product, prepared by GP-B from 13.8 mmol of propionaldehyde, was purified by column chromatography [*c*-hex/EtOAc (20:1), R_f = 0.71] to yield the product (*E/Z* mixture 96:4) as a colorless oil (1.35 g, 69%). ^1H NMR (300 MHz, CDCl_3) major diastereoisomer δ (ppm) = 1.02 (t, 3H, J = 7.6 Hz), 1.27 (t, 3H, J = 7.1 Hz), 1.80 (d, 3H, J = 1.2 Hz), 2.16 (m, 2H), 4.16 (q, 2H, J = 7.1 Hz), 6.72 (tq, 1H, J_1 = 7.4 Hz, J_2 = 1.2 Hz); ^{13}C NMR (75 MHz, CDCl_3) δ (ppm) = 12.3 (CH_3), 13.1 (CH_3), 14.4 (CH_3), 22.1 (CH_2), 60.3 (CH_2), 127.4 (CH), 144.1 (C_q), 168.4 (C_q).

(E)-Ethyl 2,4-Dimethylpent-2-enoate (1c).³² The crude product, prepared by GP-B from 5.6 mmol of isobutyraldehyde, was purified by column chromatography [*c*-hex/EtOAc (20:1), R_f = 0.68] to yield the product (*E/Z* mixture 97:3) as a yellow oil (610 mg, 70%). ^1H NMR (300 MHz, CDCl_3) major diastereoisomer δ (ppm) = 0.97 (d, 6H, J = 5.7 Hz), 1.23 (t, 3H, J = 7.1 Hz), 1.77 (d, 3H, J = 1.3 Hz), 2.70–2.48 (m, 1H), 4.16 (q, 2H, J = 7.1 Hz), 6.51 (dq, 1H, J_1 = 9.7 Hz, J_2 = 1.3 Hz); ^{13}C NMR (75 MHz, CDCl_3) δ (ppm) = 12.2 (CH_3), 14.3 (CH_3), 22.3 (CH_3), 28.1 (CH), 60.6 (CH_2), 125.8 (C_q), 149.0 (CH), 168.5 (C_q).

(E)-Ethyl 2,4,4-Trimethylpent-2-enoate (1d).³³ To a precooled (0 °C) suspension of sodium hydride (60 wt % in mineral oil, 520 mg, 13.0 mmol) in ethyl propionate (40 mmol) was added ethanol (0.7 mmol). Afterward, pivaldehyde (10 mmol, 1.1 mL) was added in portions over 30 min. After 30 min of stirring at 0 °C, the mixture was diluted with hexane, and the reaction was quenched by slow addition of saturated sodium bicarbonate, after which the mixture was further diluted with water. The layers were separated, and the aqueous phase was extracted three times with hexane. The combined extracts were dried with MgSO_4 . Hexane was evaporated under reduced pressure, and the crude product was purified by column chromatography [*c*-hex/EtOAc (8:1), R_f = 0.61] to yield the product as a colorless oil (1.27 g, 75%). ^1H NMR (300 MHz, CDCl_3) δ (ppm) = 1.15 (s, 9H), 1.27 (t, 3H, J = 7.1 Hz), 1.93 (d, 3H, J = 1.3 Hz), 4.15 (q, 2H, J = 7.1 Hz), 6.77 (q, 1H, J = 1.4 Hz); ^{13}C NMR (75 MHz, CDCl_3) δ (ppm) = 13.4 (CH_3), 14.4 (CH_3), 30.2 (CH_3), 33.0 (C), 60.7 (CH_2), 126.8 (C_q), 151.1 (CH), 169.4 (C_q).

(E)-Ethyl 2-Methyl-2,4-pentadienoate (1e).³⁴ The crude product, prepared by GP-B from 38 mmol of acrolein, was purified by column chromatography [*c*-hex/EtOAc (3:1), R_f = 0.70] to yield the product (*E/Z* mixture 96:4) as a colorless oil (4.25 g, 80%). ^1H NMR (300 MHz, CDCl_3) major diastereoisomer δ (ppm) = 1.31 (t, 3H, J = 7.1 Hz), 1.96 (d, 3H, J = 0.6 Hz), 4.22 (q, 2H, J = 7.1 Hz), 5.45 (d, 1H, J = 10.0 Hz), 5.56 (d, 1H, J = 16.8 Hz), 6.66 (m, 1H), 7.17 (dd, 1H, J_1 = 11.4 Hz, J_2 = 0.6 Hz); ^{13}C NMR (75 MHz, CDCl_3) δ (ppm) = 12.7 (CH_3), 14.4 (CH_3), 60.7 (CH_2), 124.1 (CH_2), 128.3 (C_q), 132.3 (CH), 138.3 (CH), 168.4 (C_q).

(2E,4E)-Ethyl 2-Methyl-2,4-hexadienoate (1f).³⁵ The crude product, prepared by GP-B from 38 mmol of crotonaldehyde, was purified by column chromatography [*c*-hex/EtOAc (3:1), R_f = 0.61] to yield the product (*E/Z* mixture 93:7) as a colorless oil (4.11 g, 70%). ^1H NMR (300 MHz, CDCl_3) δ (ppm) = 1.27 (t, 3H, J = 7.1 Hz), 1.84 (d, 3H, J = 6.8 Hz), 1.89 (s, 3H), 4.17 (q, 2H, J = 7.1 Hz), 6.05 (dq, 1H, J_1 = 14.4 Hz, J_2 = 6.8 Hz), 6.33 (ddd, 1H, J_1 = 14.4 Hz, J_2 = 11.3 Hz, J_3 = 1.5 Hz), 7.12 (d, 1H, J = 11.2 Hz); ^{13}C NMR (75 MHz, CDCl_3) δ (ppm) = 12.7 (CH_3), 14.4 (CH_3), 18.8 (CH_3), 60.5 (CH_2), 125.0 (C_q), 127.5 (CH), 137.0 (CH), 138.5 (CH), 168.7 (C_q).

(E)-Ethyl 2,4-Dimethyl-2,4-pentadienoate (1g).³⁸ The crude product, prepared by GP-B from 32 mmol of methacrolein, was

purified by column chromatography [*c*-hex/EtOAc (3:1), R_f = 0.64] to yield the product as a colorless oil (4.31 g, 88%). ^1H NMR (300 MHz, CDCl_3) δ (ppm) = 1.30 (t, 3H, J = 7.1 Hz), 1.93 (s, 3H), 2.02 (d, 3H, J = 1.2 Hz), 4.21 (q, 2H, J = 7.1 Hz), 5.07 (s, 1H), 5.21 (s, 1H), 7.11 (q, 1H, J = 1.2 Hz); ^{13}C NMR (75 MHz, CDCl_3) δ (ppm) = 13.9 (CH_3), 14.3 (CH_3), 22.0 (CH_3), 60.6 (CH_2), 119.7 (CH_2), 127.7 (C_q), 140.4 (CH), 140.8 (C_q), 168.8 (C_q).

(2E,4E)-Ethyl 4-Methyl-2,4-hexadienoate (E,E-1h).³⁷ The crude product, prepared by GP-A from 23.8 mmol of (*E*)-2-methyl-2-butenal, was purified by column chromatography [*c*-hex/EtOAc (70:1), R_f = 0.55] to yield the product as a colorless oil (3.05 g, 83%). ^1H NMR (300 MHz, CDCl_3) δ (ppm) = 1.25 (t, 3H, J = 7.1 Hz), 1.72 (s, 3H), 1.76 (d, 3H, J = 7.2 Hz), 4.16 (q, 2H, J = 7.1 Hz), 5.73 (d, 1H, J = 17.5 Hz), 5.93 (q, 1H, J = 7.1 Hz), 7.27 (d, 1H, J = 15.7 Hz); ^{13}C NMR (75 MHz, CDCl_3) δ (ppm) = 11.8 (CH_3), 14.4 (CH_3), 14.6 (CH_3), 60.1 (CH_2), 115.3 (CH), 133.7 (C_q), 136.31 (CH), 149.5 (CH), 167.7 (C_q).

(2E,4Z)-Ethyl 4-Methyl-2,4-hexadienoate (E,Z-1h). The crude product, prepared by GP-A from 3.51 mmol of (*Z*)-2-methyl-2-butenal, was purified by column chromatography [*c*-hex/EtOAc (70:1), R_f = 0.4] to yield the product as a colorless oil (373 mg, 69%). ^1H NMR (300 MHz, CDCl_3) δ (ppm) = 1.28 (t, 3H, J = 7.1 Hz), 1.81 (s, 3H), 1.83 (d, 3H), 4.19 (q, 2H, J = 7.1 Hz), 5.78 (q, 1H, J = 6.5 Hz), 5.84 (d, 1H, J = 15.7 Hz), 7.75 (d, 1H, J = 15.7 Hz); ^{13}C NMR (75 MHz, CDCl_3) δ (ppm) = 13.8 (CH_3), 14.4 (CH_3), 20.0 (CH_3), 60.3 (CH_2), 117.9 (CH), 131.6 (C_q), 133.8 (CH), 140.8 (CH), 167.7 (C_q).

(E,E)-Ethyl 2,4-Dimethylhexa-2,4-dienoate (E,E-1i).³⁸ The crude product, prepared by GP-B from 23.8 mmol of (*E*)-2-methyl-2-butenal, was purified by column chromatography [*c*-hex/EtOAc (10:1), R_f = 0.65] to yield the product as a colorless oil (2.20 g, 55%). ^1H NMR (300 MHz, CDCl_3) δ (ppm) = 1.28 (t, 3H, J = 7.1 Hz), 1.72 (d, 3H, J = 6.9 Hz), 1.81 (s, 3H), 1.98 (s, 3H), 4.18 (q, 2H, J = 7.1 Hz), 5.69 (q, 1H, J = 7.0 Hz), 7.10 (s, 1H); ^{13}C NMR (75 MHz, CDCl_3) δ (ppm) = 14.0 (CH_3), 14.1 (CH_3), 14.4 (CH_3), 16.0 (CH_3), 60.6 (CH_3), 125.0 (C_q), 130.9 (CH), 133.2 (C_q), 143.0 (CH), 169.3 (C_q).

(E,Z)-Ethyl 2,4-Dimethylhexa-2,4-dienoate (E,Z-1i). The crude product, prepared by GP-B from 14.7 mmol of (*Z*)-2-methyl-2-butenal, was purified by column chromatography [*c*-hex/EtOAc (20:1), R_f = 0.72] to yield the product as a colorless oil (373 mg, 69%). ^1H NMR (300 MHz, CDCl_3) δ (ppm) = 1.31 (t, 3H, J = 7.1 Hz), 1.54 (d, 3H), 1.81 (s, 3H), 1.82 (s, 3H), 4.47 (q, 2H, J = 7.1 Hz), 5.47 (q, 1H, J = 6.9 Hz), 7.13 (s, 1H); ^{13}C NMR (75 MHz, CDCl_3) δ (ppm) = 14.1 (CH_3), 14.4 (CH_3), 15.1 (CH_3), 16.0 (CH_3), 60.7 (CH_3), 125.4 (CH), 128.1 (C_q), 132.2 (C_q), 138.8 (CH), 168.5 (C_q).

(E)-2-Methyl-4-phenyl-1,3-butadiene (1j).³⁹ The crude product, prepared by GP-A from 14.3 mmol of acrolein, was purified by column chromatography [*c*-hex/EtOAc (100:1), R_f = 0.45] to yield the product as a colorless oil (1.75 g, 85%). ^1H NMR (300 MHz, CDCl_3) δ (ppm) = 2.00 (s, 3H), 5.12 (s, 2H), 6.56 (d, 1H, J = 16.4 Hz), 6.91 (d, 1H, J = 16.4 Hz), 7.25 (t, 1H, J = 7.3 Hz), 7.3 (t, 2H, J = 7.3 Hz), 7.56 (d, 2H, J = 7.8 Hz); ^{13}C NMR (75 MHz, CDCl_3) δ (ppm) = 18.7 (CH_3), 117.5 (CH_2), 126.6 (CH), 127.6 (CH), 126.7 (CH), 128.8 (CH), 131.9 (CH), 134.0 (C_q), 145.9 (C_q).

(1E,3E)-3-Methyl-1-phenyl-1,3-pentadiene (1k).⁴⁰ The crude product, prepared by GP-A from 23.8 mmol of (*E*)-2-methyl-2-butenal, was purified by column chromatography [*c*-hex/EtOAc (20:1), R_f = 0.53] to yield the product as a colorless oil (2.82 g, 75%). ^1H NMR (300 MHz, CDCl_3) δ (ppm) = 1.80 (d, 3H, J = 7.0 Hz), 1.87 (s, 3H), 5.72 (q, 1H, J = 7.0 Hz), 6.45 (d, 1H, J = 16.1 Hz), 6.82 (d, 1H, J = 16.1 Hz), 7.15–7.44 (m, 5H); ^{13}C NMR (75 MHz, CDCl_3) δ (ppm) = 12.3 (CH_3), 14.3 (CH_3), 125.5 (CH), 126.4 (C_q), 127.0 (CH), 128.4 (CH), 128.8 (CH), 134.2 (CH), 134.9 (C_q), 138.3 (C_q).

(2E,4E)-4-Methyl-2-phenyl-2,4-hexadiene (1l).⁴⁰ The crude product, prepared by GP-B from 23.8 mmol of (*E*)-2-methyl-2-butenal, was purified by column chromatography [*c*-hex/EtOAc (20:1), R_f = 0.55] to yield the product as a colorless oil (2.74 g, 73%). ^1H NMR (300 MHz, CDCl_3) δ (ppm) = 1.83 (d, 3H, J = 6.9 Hz), 1.91 (s, 3H), 2.27

(s, 3H), 5.72 (q, 1H, $J = 6.9$ Hz), 6.32 (s, 1H), 7.26–7.54 (m, 5H); ^{13}C NMR (75 MHz, CDCl_3) δ (ppm) = 13.9 (CH_3), 16.9 (CH_3), 17.6 (CH_3), 125.0 (CH), 126.0 (CH), 126.7 (CH), 128.3 (CH), 132.0 (CH), 134.0 (C_q), 134.0 (C_q), 144.7 (C_q).

Photooxygenation, Reduction, and Oxygen Transfer. General Procedure for Photooxygenations (GP-C). A 3 mL aliquot of a CDCl_3 stock solution, 2×10^{-4} M in the photosensitizer TPP and 0.2 M in the corresponding diene, was added to a Schlenk tube equipped with a magnetic stirrer. During irradiation with a 50 W white LED lamp at room temperature, oxygen was bubbled through the solution. The reaction was controlled by TLC and NMR spectroscopy. After complete conversion, the solvent was evaporated under reduced pressure at 5 °C. The conversion and isomeric ratio were determined from the crude reaction mixture.

General Procedure for Reductions (GP-D). To the hydroperoxide-containing solution from GP-C, dimethyl sulfide (5 equiv with respect to the calculated substrate amount in the photooxygenation reaction) was added at 0 °C. The mixture was allowed to stir for 12 h at room temperature in the dark. The solvent was removed under reduced pressure, and the crude product was purified by column chromatography. Compounds **2b–d** from the kinetic studies were characterized by NMR analyses only.

Ethyl 3-Hydroperoxy-2-methylenebutanoate (2a).²¹ ^1H NMR (300 MHz, CDCl_3) δ (ppm) = 0.89 (t, 3H, $J = 7.4$ Hz), 1.26 (t, 3H, $J = 7.1$ Hz), 1.81–1.46 (m, 2H), 4.18 (q, 2H, $J = 7.1$ Hz), 4.92 (t, 1H, $J = 6.6$ Hz), 5.86 (s, 1H), 6.34 (s, 1H), 9.10 (s, 1H); ^{13}C NMR (75 MHz, CDCl_3) δ (ppm) = 14.0 (CH_3), 18.5 (CH_3), 61.0 (CH_2), 79.2 (CH), 125.7 (CH_2), 140.6 (C_q), 166.4 (C_q).

Ethyl 3-Hydroperoxy-2-methylenepentanoate (2b). ^1H NMR (300 MHz, CDCl_3) δ (ppm) = 1.26 (t, 3H, $J = 7.1$ Hz), 1.29 (d, 3H, $J = 6.6$ Hz), 4.18 (q, 2H, $J = 7.1$ Hz), 4.92 (q, 1H, $^3J_{\text{HH}} = 6.6$ Hz), 5.88 (s, 1H), 6.30 (s, 1H), 9.16 (s, 1H); ^{13}C NMR (75 MHz, CDCl_3) δ (ppm) = 9.8 (CH_3), 14.1 (CH_3), 26.0 (CH_2), 61.4 (CH_2), 84.6 (CH), 126.1 (CH_2), 139.6 (C_q), 166.5 (C_q).

Ethyl 3-Hydroperoxy-4-methyl-2-methylenepentanoate (2c). ^1H NMR (300 MHz, CDCl_3) δ (ppm) = 0.93 (d, 3H, $J = 3.2$ Hz), 0.95 (d, 3H, $J = 3.1$ Hz), 1.26 (t, 3H, $J = 7.1$ Hz), 2.01–1.89 (m, 1H), 4.18 (q, 2H, $J = 7.1$ Hz), 4.68 (d, 1H, $J = 6.6$ Hz), 5.87 (s, 1H), 6.42 (s, 1H), 8.48 (s, 1H); ^{13}C NMR (75 MHz, CDCl_3) δ (ppm) = 14.1 (CH_3), 17.9 (CH_3), 19.1 (CH_3), 31.4 (CH), 60.2 (CH_2), 84.6 (CH), 126.4 (CH_2), 139.6 (C_q), 166.7 (C_q).

Ethyl 3-Hydroperoxy-4,4-dimethyl-2-methylenepentanoate (2d). ^1H NMR (300 MHz, CDCl_3) δ (ppm) = 0.89 (s, 9H), 1.25 (t, 3H, $J = 6.8$ Hz), 4.21 (q, 2H, $J = 7.1$ Hz), 4.82 (s, 1H), 5.84 (s, 1H), 6.43 (s, 1H), 8.55 (s, 1H); ^{13}C NMR (75 MHz, CDCl_3) δ (ppm) = 14.1 (CH_3), 25.9 (CH_3), 35.4 (C_q), 61.5 (CH_2), 89.4 (CH), 124.8 (CH_2), 138.8 (C_q), 167.4 (C_q).

Ethyl 3-Hydroxy-2-methylenepent-4-enoate (16e). The crude product, prepared by GP-C and GP-D from 5.71 mmol of **1e**, was purified by column chromatography [*c*-hex/EtOAc (3:1), $R_f = 0.48$] to yield the alcohol as a yellow oil (120 mg, 14%) and the endoperoxide [*c*-hex/EtOAc (3:1), $R_f = 0.61$] as a colorless oil (96 mg, 10%). ^1H NMR (300 MHz, CDCl_3) δ (ppm) = 1.24 (t, 3H, $J = 7.1$ Hz), 3.03 (s, 1H), 4.17 (q, 2H, $J = 7.1$ Hz), 4.89 (d, 1H, $J = 4.8$ Hz), 5.12 (d, 1H, $J = 10.5$ Hz), 5.27 (d, 1H, $J = 17.2$ Hz), 5.78 (s, 1H), 5.89 (m, 1H), 6.19 (s, 1H); ^{13}C NMR (75 MHz, CDCl_3) δ (ppm) = 13.8 (CH_3), 60.5 (CH_2), 71.8 (CH), 115.6 (CH_2), 125.1 (CH_2), 137.9 (CH), 141.1 (C_q), 170.8 (C_q); IR (film) ν (cm^{-1}) = 3427, 2922, 2363, 1707, 1696, 1636; HRMS (EI) calcd for $\text{C}_7\text{H}_{11}\text{O}_2$ m/z 127.075 [$\text{M} - \text{CH}_2\text{O}$]⁺, found 127.074.

Ethyl 3-Methyl-3,6-Dihydro-1,2-dioxine-3-carboxylate (3). ^1H NMR (300 MHz, CDCl_3) δ (ppm) = 1.27 (t, 3H, $J = 7.1$ Hz), 1.39 (s, 3H), 4.21 (q, 2H, $J = 7.1$ Hz), 4.29–4.23 (ddd, 1H, $J_1 = 16.6$ Hz, $J_2 = 3.8$ Hz, $J_3 = 1.2$ Hz), 4.75 (dt, 1H, $J_1 = 16.6$ Hz, $J_2 = 1.2$ Hz), 6.01 (ddd, 1H, $J_1 = 10.2$ Hz, $J_2 = 3.8$ Hz, $J_3 = 1.2$ Hz), 6.09 (dt, 1H, $J_1 = 10.2$ Hz, $J_2 = 1.6$ Hz); ^{13}C NMR (75 MHz, CDCl_3) δ (ppm) = 13.7 (CH_3), 22.0 (CH_3), 61.6 (CH_2), 69.3 (CH_2), 80.6 (C_q), 124.7 (CH), 127.7 (CH), 171.6 (C_q); IR (film) ν (cm^{-1}) = 3564, 2986, 2358, 1727, 1699, 1683, 1538, 1445, 1371. Anal. Calcd for $\text{C}_8\text{H}_{12}\text{O}_4$: C, 55.81; H, 7.02. Found: C, 55.57; H, 7.03.

(E)-Ethyl 3-Hydroxy-2-methylenehex-4-enoate (16f). The crude product, prepared by GP-C and GP-D from 3.25 mmol of **1f**, was purified by column chromatography [*c*-hex/EtOAc (3:1), $R_f = 0.56$] to yield the product as a yellow oil (90 mg, 16%). ^1H NMR (300 MHz, CDCl_3) δ (ppm) = 1.29 (t, 3H, $J = 7.1$ Hz), 1.69 (d, 3H, $J = 6.4$ Hz), 2.73 (s, 1H), 4.21 (q, 2H, $J = 7.1$ Hz), 4.87 (d, 1H, $J = 6.5$ Hz), 5.56 (dd, 1H, $J_1 = 15.3$ Hz, $J_2 = 6.5$ Hz), 5.77–5.65 (m, 1H), 5.79 (s, 1H), 6.20 (s, 1H); ^{13}C NMR (75 MHz, CDCl_3) δ (ppm) = 13.7 (CH_3), 17.7 (CH_3), 60.9 (CH_2), 72.1 (CH), 124.9 (CH_2), 128.0 (CH), 130.7 (CH), 141.9 (C_q), 166.5 (C_q); IR (film) ν (cm^{-1}) = 3427, 2922, 2363, 1707, 1696, 1636.

Ethyl 3,6-Dimethyl-3,6-dihydro-1,2-dioxine-3-carboxylate (4). The crude product, prepared by GP-C and GP-D from 3.25 mmol of **1f**, was purified by column chromatography [*c*-hex/EtOAc (3:1), $R_f = 0.64$] to yield the product as a yellow oil (55 mg, 9%). ^1H NMR (300 MHz, CDCl_3) δ (ppm) = 1.13 (d, 3H, $J = 6.8$ Hz), 1.27 (t, 3H, $J = 7.1$ Hz), 1.38 (s, 3H), 4.22 (q, 2H, $J = 7.1$ Hz), 4.78 (m, 1H, $J = 6.8$ Hz), 5.86 (dd, 1H, $J_1 = 10.2$ Hz, $J_2 = 0.6$ Hz), 6.03 (dd, 1H, $J_1 = 10.1$ Hz, $J_2 = 2.0$ Hz); ^{13}C NMR (75 MHz, CDCl_3) δ (ppm) = 14.2, 17.1, 22.0, 60.1, 73.8, 80.1, 127.4, 129.9, 171.8; IR (film) ν (cm^{-1}) = 3018, 2358, 1726, 1683, 1445, 1369; HRMS (EI) calcd for $\text{C}_9\text{H}_{14}\text{O}_4$ m/z 141.0552 [$\text{M} - \text{C}_2\text{H}_5\text{O}$]⁺, found 141.0550.

Ethyl 3-Hydroxy-4-methyl-2-methylenepent-4-enoate (16g). The crude product, prepared by GP-C and GP-D from 6.49 mmol of **1g**, was purified by column chromatography [*c*-hex/EtOAc (3:1), $R_f = 0.53$] to yield the product as a yellow oil (76 mg, 7%). ^1H NMR (300 MHz, CDCl_3) δ (ppm) = 1.30 (t, 3H, $J = 7.1$ Hz), 1.72 (s, 3H), 2.75 (s, 1H), 4.22 (q, 2H, $J = 7.1$ Hz), 4.90 (s, 1H), 4.97 (s, 1H), 5.08 (s, 1H), 5.83 (s, 1H), 6.30 (s, 1H); ^{13}C NMR (75 MHz, CDCl_3) δ (ppm) = 14.3 (CH_3), 19.0 (CH_3), 61.1 (CH_2), 74.8 (CH), 112.6 (CH_2), 126.1 (CH_2), 140.6 (C_q), 144.7 (C_q), 166.7 (C_q); IR (film) ν (cm^{-1}) = 3445, 3078, 2979, 2936, 1910, 1710, 1627; HRMS (EI) calcd for $\text{C}_8\text{H}_{13}\text{O}_2$ m/z 141.091 [$\text{M} - \text{CH}_2\text{O}$]⁺, found 141.091.

Ethyl 3,5-Dimethyl-3,6-dihydro-1,2-dioxine-3-carboxylate (5). The crude product, prepared by GP-C and GP-D from 6.49 mmol of **1g**, was purified by column chromatography [*c*-hex/EtOAc (3:1), $R_f = 0.70$] to yield the product as a white solid (354 mg, 37%). ^1H NMR (300 MHz, CDCl_3) δ (ppm) = 1.28 (t, 3H, $J = 7.1$ Hz), 1.39 (s, 3H), 1.74 (s, 3H), 4.09 (d, 1H, $J = 16.0$ Hz), 4.31–4.14 (m, 2H), 4.62 (d, 1H, $J = 16.0$ Hz), 5.77 (m, 1H); ^{13}C NMR (75 MHz, CDCl_3) δ (ppm) = 14.2 (CH_3), 18.0 (CH_3), 22.4 (CH_3), 61.5 (CH_2), 72.4 (CH_2), 80.4 (C_q), 121.6 (CH), 132.7 (C_q), 171.9 (C_q); IR (film) ν (cm^{-1}) = 2988, 1715, 1473, 1447, 1368; HRMS (EI) calcd for $\text{C}_9\text{H}_{14}\text{O}_4$ m/z 141.0552 [$\text{M} - \text{C}_2\text{H}_5\text{O}$]⁺, found 141.056. Anal. Calcd for $\text{C}_9\text{H}_{14}\text{O}_4$: C, 58.05; H, 7.58. Found: C, 57.93; H, 7.57.

(E)-Ethyl 5-Hydroperoxy-4-methylenehex-2-enoate (7). Photooxygenation of 180 mg (1.12 mmol) of **1h** for 3.5 h according to GP-C led to the exclusive formation of hydroperoxide **7** (characterized by NMR and IR only). ^1H NMR (300 MHz, CDCl_3) δ (ppm) = 1.31 (t, 3H, $J = 7.2$ Hz), 1.37 (d, 3H, $J = 6.6$ Hz), 4.22 (q, 2H, $J = 7.1$ Hz), 4.82 (q, 1H, $J = 6.5$ Hz), 5.59 (2H, d, $J = 4.6$ Hz), 6.13 (d, 1H, $J = 16.1$ Hz), 7.30 (d, 1H, $J = 16.1$ Hz), 8.70 (s, 1H); ^{13}C NMR (75 MHz, CDCl_3) δ (ppm) = 14.5 (CH_3), 18.5 (CH_3), 60.9 (CH_2), 81.2 (CH), 119.5 (CH), 123.1 (CH_2), 143.5 (CH), 144.6 (C_q), 167.3 (C_q); IR (film) ν (cm^{-1}) = 3284 (s), 2983 (m), 2935 (m), 2841 (s), 1702 (s), 1618 (s).

(E)-Ethyl 5-Hydroperoxy-2-methyl-4-methylenehex-2-enoate (9). Photooxygenation of 200 mg (1.19 mmol) of **1i** for 3 h according to GP-C led to the exclusive formation of hydroperoxide **9** (characterized by NMR and IR only). ^1H NMR (300 MHz, CDCl_3) δ (ppm) = 1.25 (d, 3H, $J = 6.6$ Hz), 1.29 (t, 3H, $J = 7.1$ Hz), 2.00 (s, 3H), 4.21 (q, 2H, $J = 7.0$ Hz), 4.82 (q, 1H, $J = 6.6$ Hz), 5.3 (1H, s), 5.51 (1H, s), 7.12 (t, 1H, $J = 1.2$ Hz), 8.42 (s, 1H). ^{13}C NMR (150 MHz, CDCl_3) δ (ppm) = 14.3 (CH_3), 14.3 (CH_3), 17.9 (CH_3), 61.1 (CH_2), 84.3 (CH), 118.7 (CH_2), 131.1 (C_q), 135.4 (CH), 144.4 (C_q), 168.5 (C_q); IR ν (cm^{-1}) = 3222, 2972, 2875, 2361, 1707, 1621.

3,6-Dihydro-5-methyl-3-phenyl-1,2-dioxine (11). Photooxygenation of 100 mg (0.69 mmol) of **1j** for 2 h according to GP-C led to the formation of 120 mg (98%) of endoperoxide **11**. ^1H NMR (300 MHz, CDCl_3) δ (ppm) = 1.83 (s, 3H), 4.42 (d, 1H, $J = 15.8$ Hz), 4.57 (d,

1H, $J = 15.8$ Hz), 5.59 (s, 1H), 5.80 (s, 1H), 7.35–7.42 (m, 5H); ^{13}C NMR (75 MHz, CDCl_3) δ (ppm) = 18.38 (CH_3), 73.13 (CH_2), 80.52 (CH), 120.90 (CH), 128.7 (CH), 128.8 (CH), 128.9 (C_q), 132.6 (C_q), 137.9 (C_q); HRMS (EI) calcd for $\text{C}_{11}\text{H}_{12}\text{O}_2$ m/z 176.0837 [M] $^+$, found 176.0839.

3,6-Dihydro-5-(1-hydroperoxyethyl)-3-phenyl-1,2-dioxine (12). Photooxygenation of 100 mg (0.50 mmol) of **1k** for 12 h according to GP-C led to the formation of 105 mg (95%) of hydroperoxyendoperoxide **12** (dr = 50:50) (characterized by NMR and IR only). ^1H NMR (600 MHz, CDCl_3) diastereoisomers A/B δ (ppm) = 1.37 (d, 3H, $J = 6.7$ Hz)/1.45 (d, 3H, $J = 6.7$ Hz), 4.56–4.91 (m, 3H/3H), 5.58 (s, 1H)/5.69 (s, 1H), 6.06 (s, 1H)/6.10 (s, 1H), 7.32–7.41 (m, 5H/5H), 8.37 (s, 1H/1H); ^{13}C NMR (150 MHz, CDCl_3) δ (ppm) = 16.9/17.0 (CH_3), 69.3/69.3 (CH_2), 80.2/80.4 (CH), 81.6/81.9 (CH), 124.0/124.6 (CH), 128.4–129.3 (C_{aryl}); IR ν (cm^{-1}) = 3418, 2982, 2893, 2328, 1636.

3,6-Dihydro-5-(1-hydroperoxyethyl)-3-methyl-3-phenyl-1,2-dioxine (14). Photooxygenation of 100 mg (0.50 mmol) of **1l** for 10 h according to GP-C resulted in the formation of hydroperoxyendoperoxide **14** (105 mg, 90%; dr = 68:32) (characterized by NMR and IR only). ^1H NMR (600 MHz, CDCl_3) diastereoisomers A/B δ (ppm) = 1.33–1.41 (m, 6H), 1.57 (s, 3H)/1.58 (s, 3H), 4.42–4.81 (m, 3H/3H), 6.27 (s, 1H)/6.33 (s, 1H), 7.23–7.53 (m, 5H/5H), 8.28 (s, 1H/1H); ^{13}C NMR (150 MHz, CDCl_3) δ (ppm) = 16.7/17.0 (CH_3), 26.0/26.3 (CH_3), 68.7/68.9 (CH_2), 80.8/81.0 (C_q), 81.5/81.9 (CH), 125.5/125.9 (CH), 127.6/127.7 (CH), 128.2/128.4 (CH), 134.5/134.6 (C_q); IR ν (cm^{-1}) = 3888, 3000, 2912, 1620.

(E)-Ethyl 5-Hydroxy-4-methylenehex-2-enoate (17). The crude product, prepared by GP-D from 180 mg of **7**, was purified by column chromatography [*c*-hex/EtOAc (2:1), $R_f = 0.28$] to yield the product as a colorless oil (86 mg, 45%). ^1H NMR (300 MHz, CDCl_3) δ (ppm) = 1.27 (t, 3H, $J = 7.2$ Hz), 1.34 (d, 3H, $J = 6.5$ Hz), 2.37 (s, 1H), 4.18 (q, 2H, $J = 7.1$ Hz), 4.56 (q, 1H, $J = 6.4$ Hz), 5.42 (1H, s), 5.60 (1H, s), 6.01 (d, 1H, $J = 16.2$ Hz), 7.27 (d, 1H, $J = 16.2$ Hz); ^{13}C NMR (75 MHz, CDCl_3) δ (ppm) = 14.4 (CH_3), 23.1 (CH_3), 60.7 (CH_2), 67.2 (CH), 118.9 (CH), 120.9 (CH_2), 144.1 (CH), 148.7 (C_q), 167.3 (C_q); IR (film) ν (cm^{-1}) = 3430, 2981, 2929, 2841, 1688, 1626; HRMS (EI) calcd for $\text{C}_9\text{H}_{14}\text{O}_3$ m/z 170.0942 [M] $^+$, found 170.0926.

(E)-Ethyl 5-Hydroxy-2-methyl-4-methylenehex-2-enoate (18). The crude product, prepared by GP-D from 226 mg of **9**, was purified by column chromatography [*c*-hex/EtOAc (2:1), $R_f = 0.33$] to yield the product as a colorless oil (117 mg, 49%). ^1H NMR (300 MHz, CDCl_3) δ (ppm) = 1.22 (d, 3H, $J = 6.5$ Hz), 1.25 (t, 3H, $J = 7.1$ Hz), 1.93 (d, 3H, $J = 1.5$ Hz), 2.71 (s, 1H), 4.15 (q, 2H, $J = 7.1$ Hz), 4.31 (q, 1H, $J = 6.4$ Hz), 5.02 (1H, s), 5.43 (1H, s), 7.04 (t, 1H, $J = 1.2$ Hz); ^{13}C NMR (75 MHz, CDCl_3) δ (ppm) = 14.3 (CH_3), 14.3 (CH_3), 22.5 (CH_3), 60.9 (CH_2), 70.6 (CH), 115.1 (CH_2), 130.4 (C_q), 136.4 (CH), 148.4 (C_q), 168.4 (C_q); IR (film) ν (cm^{-1}) = 3427, 2980, 2933, 2875, 2358, 2341, 1708, 1693, 1631; HRMS (EI) calcd for $\text{C}_{10}\text{H}_{16}\text{O}_3$ m/z 184.1091 [M] $^+$, found 184.1095.

Ethyl 5-(1-Hydroperoxyethyl)-3,6-dihydro-1,2-dioxine-3-carboxylate (19). Photooxygenation of 100 mg (0.46 mmol) of **1i** for 36 h according to GP-C led to the exclusive formation of hydroperoxyendoperoxide **19** (86 mg, 75%; dr = 50:50). ^1H NMR (300 MHz, CDCl_3) diastereoisomers A/B δ (ppm) = 1.24–1.37 (m, 6H/6H), 4.13–5.08 (m, 5H/5H, $\text{CH}_2\text{--CH}_3$, $\text{CH}_2\text{--O--O}$, CH--OOH), 6.12 (s, 1H/1H); ^{13}C NMR (75 MHz, CDCl_3) diastereoisomers A/B δ (ppm) = 14.1/14.2 (CH_3), 16.2/16.2 (CH_3), 61.8/61.9 (CH_2), 69.1/69.2 (CH_2), 76.4/76.5 (CH), 81.0/81.2 (CH), 118.5/118.8 (CH), 138.2/138.3 (C_q), 168.4/168.6 (C_q); IR (film) ν (cm^{-1}) = 3429, 2978, 2349, 1731, 1720, 1672.

Ethyl 5-(1-Hydroperoxyethyl)-3-methyl-3,6-dihydro-1,2-dioxine-3-carboxylate (20). Photooxygenation of 100 mg (0.61 mmol) of **1i** for 26 h according to GP-C led to the exclusive formation of 112 mg of hydroperoxyendoperoxide **20** (dr = 50:50). ^1H NMR (600 MHz, CDCl_3) diastereoisomers A/B δ (ppm) = 1.22–1.30 (m, 6H/6H), 1.37 (s, 3H)/1.40 (s, 3H), 4.14–4.21 (m, 2H/2H), 4.35 (d, 1H, $J = 16.2$ Hz)/4.36 (d, 1H, $J = 16.3$ Hz), 4.51–4.56 (m, 1H/1H), 4.70–4.78 (m, 1H/1H), 5.99 (s, 1H)/6.00 (s, 1H), 9.04 (br s, 1H)/9.07 (br s, 1H, OOH); ^{13}C NMR (150 MHz, CDCl_3) diastereoisomers A/B δ

(ppm) = 14.1/14.1 (CH_3), 16.7/17.0 (CH_3), 21.9/22.1 (CH_3), 61.8/61.8 (CH_2), 68.8/68.8 (CH_2), 80.3/80.3 (C_q), 80.8/81.3 (CH), 123.7/124.6 (CH), 136.8/136.9 (C_q), 171.9/171.9 (C_q); IR (film) ν (cm^{-1}) = 3440, 2988, 2358, 2330, 1732, 1716, 1681, 1635.

Ethyl 5-(1-Hydroxyethyl)-3,6-dihydro-1,2-dioxine-3-carboxylate (21). The crude product, prepared by GP-D from 150 mg of **19**, was purified by column chromatography [*c*-hex/EtOAc (2:1), $R_f = 0.45$] to yield the product as a colorless oil (107 mg, 70%). ^1H NMR (600 MHz, CDCl_3) diastereoisomers A/B δ (ppm) = 1.31–1.34 (m, 3H/3H), 1.36 (d, 2H, $J = 6.5$ Hz)/1.36 (d, 2H, $J = 6.5$ Hz), 4.25–4.32 (m, 2H/2H), 4.38 (q, 1H, $J = 6.5$ Hz)/4.44 (q, 1H, $J = 6.5$ Hz), 4.48 (d, 1H, $J = 16.4$ Hz)/4.54 (d, 1H, $J = 16.6$ Hz), 4.77 (d, 1H, $J = 16.4$ Hz)/4.83 (d, 1H, $J = 16.6$ Hz), 4.97 (s, 1H)/5.00 (s, 1H), 6.06–6.08 (m, 1H)/6.08–6.10 (m, 1H); ^{13}C NMR (150 MHz, CDCl_3) diastereoisomers A/B δ (ppm) = 14.3/14.3 (CH_3), 21.7/21.9 (CH_3), 61.9/61.9 (CH_2), 67.9/68.3 (CH), 69.3/69.6 (CH_2), 76.6/76.7 (CH), 115.2/115.8 (CH), 141.7/141.8 (C_q); IR (film) ν (cm^{-1}) = 3415, 2988, 2940, 2333, 2330, 2299, 1744, 1700, 1688; HRMS (EI) calcd for $\text{C}_{10}\text{H}_{14}\text{O}_5$ m/z 202.0832 [M] $^+$, found 202.0831.

Ethyl 5-(1-Hydroxyethyl)-3-methyl-3,6-dihydro-1,2-dioxine-3-carboxylate (22). The crude product, prepared by GP-D from 200 mg of **20**, was purified by column chromatography [*c*-hex/EtOAc (2:1), $R_f = 0.50$] to yield the product as a colorless oil (180 mg, 75%). ^1H NMR (600 MHz, CDCl_3) diastereoisomers A/B δ (ppm) = 1.27 (t, 3H/3H, $J = 7.1$ Hz), 1.30 (d, 3H, $J = 3.8$ Hz)/1.32 (d, 3H, $J = 3.8$ Hz), 1.39 (s, 3H)/1.40 (s, 3H), 2.35 (s, 1H/1H), 4.15–4.26 (m, 2H/2H), 4.31 (q, 1H, $J = 6.6$ Hz)/4.38 (q, 1H, $J = 6.6$ Hz), 4.32 (d, 1H, $J = 14.8$ Hz)/4.38 (d, 1H, $J = 14.8$ Hz), 4.71 (d, 1H, $J = 16.3$ Hz)/4.78 (d, 1H, $J = 16.3$ Hz), 5.95 (s, 1H)/5.95 (s, 1H); ^{13}C NMR (150 MHz, CDCl_3) diastereoisomers A/B δ (ppm) = 14.2/14.2 (CH_3), 21.6/21.9 (CH_3), 22.1/22.2 (CH_3), 61.7/61.7 (CH_2), 67.5/68.3 (CH), 68.8/69.2 (CH_2), 80.3/80.4 (C_q), 120.4/121.5 (CH), 140.4/140.5 (C_q), 171.9/171.9 (C_q); IR (film) ν (cm^{-1}) = 3420 (s_b), 2982 (w), 2936 (w), 2905 (w), 2353 (w), 2328 (w), 1732 (s), 1715 (s), 1645 (m); HRMS (ESI) calcd for $\text{C}_{10}\text{H}_{16}\text{O}_5$ m/z 239.0889 [$\text{M} + \text{Na}$] $^+$, found 239.0887.

1-(3,6-Dihydro-6-phenyl-1,2-dioxin-4-yl)ethanol (23). The crude product, prepared by GP-D from the reduction of 200 mg (1.00 mmol) of hydroperoxide **12**, was purified by column chromatography [*c*-hex/EtOAc (3:1), $R_f = 0.3$] to yield the product as a colorless oil (89 mg, 43%; dr = 68:32). ^1H NMR (500 MHz, CDCl_3) diastereoisomers A/B δ (ppm) = 1.36 (d, 3H, $J = 6.5$ Hz)/1.42 (d, 3H, $J = 6.7$ Hz), 2.34 (s, 1H/1H), 4.33–4.45 (m, 1H/1H), 4.58–4.89 (m, 2H/2H), 5.56–5.63 (m, 1H/1H), 5.94–6.02 (m, 1H), 7.33–7.38 (m, 5H/5H); ^{13}C NMR (125 MHz, CDCl_3) diastereoisomers A/B δ (ppm) = 22.0/22.0 (CH_3), 68.0/68.4 (CH), 69.4/69.6 (CH_2), 80.2/80.3 (CH), 120.1/120.6 (CH), 128.4/128.5 (CH), 128.6/128.7 (CH), 128.9/130.0 (CH), 129.0/129.0 (CH), 137.2/137.4 (C_q), 140.2/140.2 (C_q); IR (film) ν (cm^{-1}) = 3404, 3086, 3062, 3032, 2972, 2929, 2887, 2362, 2343, 1701, 1653, 1618; HRMS (ESI) calcd for $\text{C}_{12}\text{H}_{14}\text{O}_3$ m/z 229.0835 [$\text{M} + \text{Na}$] $^+$, found 229.0837.

1-(5-Phenylfuran-3-yl)ethanol (24). To a solution of compound **23** (200 mg, 1 mmol) in MeOH (5 mL) was added thiourea (2 mmol), and the mixture was stirred for 48 h. The solvent was evaporated under reduced pressure, and the crude product was purified by column chromatography [*c*-hex/EtOAc (2:1), $R_f = 0.25$] to yield the product as a yellowish oil (116 mg, 62%). ^1H NMR (300 MHz, CDCl_3) δ (ppm) = 1.54 (d, 3H, $J = 6.4$ Hz), 1.99 (s, 1H), 4.90 (q, 1H, $J = 6.4$ Hz), 6.71 (s, 1H), 7.28 (t, 1H, $J = 7.0$ Hz), 7.40 (t, 2H, $J = 7.0$ Hz), 7.42 (s, 1H), 7.68 (d, 2H, $J = 7.0$ Hz); ^{13}C NMR (75 MHz, CDCl_3) δ (ppm) = 24.1 (CH_3), 63.2 (CH), 103.9 (CH), 123.9 (C_q), 127.6 (CH), 128.8 (CH), 130.8 (C_q), 132.5 (C_q), 138.0 (CH); IR (film) ν (cm^{-1}) = 3398, 2999, 2897, 1761; HRMS (EI) calcd for $\text{C}_{12}\text{H}_{12}\text{O}_2$ m/z 188.0842 [M] $^+$, found 188.0847.

Ethyl 4-(1-Hydroxyethyl)furan-2-carboxylate (25). To an ice-cooled solution of compound **21** (190 mg, 1 mmol) in MeOH (5 mL) was added thiourea (2 mmol), and the mixture was stirred for 24 h. The solvent was evaporated under reduced pressure, and the crude product was purified by column chromatography [*c*-hex/EtOAc (1:2), $R_f = 0.4$] to yield the product as a colorless oil (62 mg, 34%). ^1H NMR

(300 MHz, CDCl₃) δ (ppm) = 1.31 (t, 3H, J = 7.1 Hz), 1.43 (d, 3H, J = 6.4 Hz), 2.17 (s, 1H), 4.29 (q, 2H, J = 7.1 Hz), 4.81 (q, 1H, J = 6.4 Hz), 7.11 (s, 1H), 7.45 (s, 1H); ¹³C NMR (75 MHz, CDCl₃) δ (ppm) = 14.3 (CH₃), 24.1 (CH₃), 61.1 (CH₂), 62.7 (CH), 116.4 (CH), 132.5 (C_q), 142.1 (C_q), 142.2 (CH), 158.8 (C_q); IR (film) ν (cm⁻¹) = 3390, 2998, 2970, 1782, 1520, 1454; HRMS (EI) calcd for C₉H₁₂O₄ m/z 184.0732 [M]⁺, found 184.0735.

(*E*)-Ethyl 3-(2-(1-Hydroxyethyl)oxiran-2-yl)acrylate (**26**).²⁵ Hydroperoxide **7** (219 mg, 1.17 mmol) was reacted with 10 mol % titanium tetrakisopropoxide (TTIP) in 20 mL of CDCl₃ for 12 h at -15 °C. The solvent was removed under reduced pressure, and the crude product was purified by column chromatography [c-hex/EtOAc (3:1), R_f = 0.3] to yield the product as a colorless oil (121 mg, 51%; dr = 88:12). ¹H NMR (300 MHz, CDCl₃) major diastereoisomer δ (ppm) = 1.22–1.30 (m, 6H), 2.40 (s, 1H), 2.65 (d, 1H, J = 5.5 Hz), 3.06 (d, 1H, J = 5.5 Hz), 3.88 (q, 1H), 4.17 (q, 2H, J = 7.1 Hz), 6.07 (d, 1H, J = 15.6 Hz), 7.05 (d, 1H, J = 15.6 Hz); ¹³C NMR (75 MHz, CDCl₃) major diastereoisomer δ (ppm) = 14.3 (CH₃), 18.9 (CH), 53.4 (CH₂), 60.8 (CH₂), 66.8 (CH), 123.1 (CH), 142.8 (CH), 166.1 (C_q); IR ν (cm⁻¹) = 3458, 2982, 2936, 2907, 1718, 1659; HRMS (ESI) calcd for C₉H₁₄O₄ m/z 209.0784 [M + Na]⁺, found 209.0783.

(*E*)-Ethyl 3-(2-(1-Hydroxyethyl)oxiran-2-yl)-2-methylacrylate (**27**).²⁵ Hydroperoxide **9** (200 mg, 1.00 mmol) was reacted with 10 mol % TTIP in 20 mL of CDCl₃ for 12 h at -15 °C. The solvent was removed under reduced pressure, and the crude product was purified by column chromatography [c-hex/EtOAc (2:1), R_f = 0.36] to yield the product as a colorless oil (90 mg, 45%; dr = 90:10). ¹H NMR (300 MHz, CDCl₃) major diastereoisomer δ (ppm) = 1.27 (d, 3H, J = 6.4 Hz), 1.30 (t, 3H, J = 7.1 Hz), 1.90 (d, 3H, J = 1.4 Hz), 2.73 (d, 1H, J = 5.3 Hz), 3.12 (d, 1H, J = 5.3 Hz), 3.88 (q, 1H, J = 6.2 Hz), 4.20 (q, 2H, J = 7.1 Hz), 6.89 (s, 1H); ¹H NMR (300 MHz, CDCl₃) minor diastereoisomer δ (ppm) = 1.27 (d, 3H, J = 6.4 Hz), 1.30 (t, 3H, J = 7.1 Hz), 1.90 (d, 3H, J = 1.4 Hz), 2.73 (d, 1H, J = 5.3 Hz), 3.12 (d, 1H, J = 5.3 Hz), 3.88 (q, 1H, J = 6.2 Hz), 4.20 (q, 2H, J = 7.1 Hz), 6.89 (s, 1H); ¹³C NMR (75 MHz, CDCl₃) major diastereoisomer δ (ppm) = 14.2 (CH₃), 14.2 (CH₃), 18.5 (CH₃), 49.9 (CH₂), 61.1 (CH₂), 66.9 (CH), 133.8 (CH), 134.0 (CH), 167.4 (C_q); ¹³C NMR (75 MHz, CDCl₃) minor diastereoisomer δ (ppm) = 13.9 (CH₃), 13.9 (CH₃), 19.6 (CH₃), 51.7 (CH₂), 61.0 (CH₂), 68.4 (CH), 134.5 (CH), 134.5 (C_q), 167.5 (C_q); IR ν (cm⁻¹) = 3470, 2984, 2940, 2925, 1735, 1671, 1655, 1643.

■ COMPUTATIONAL DETAILS

All of the computations in this work were carried out with the program package TURBOMOLE 6.3³¹ employing the unrestricted TPSS functional (exchange and correlation)²⁸ and the contracted TZVP basis from the Ahlrich group.²⁹ All of the structure geometries were fully optimized using quasi-Newton–Raphson methods and rationalized by analytic frequency calculations. Zero-point energy corrections were omitted for all activation barriers, since the harmonic approximation caused errors in the vibrational contributions from the intermediates BR_a and BR_b (see Scheme 11) in range of 0.3 kcal/mol. The multipole-accelerated resolution of identity approximation was used to reduce the computational cost without producing qualitative errors; the grid size for numerical integration was set to mS.

■ ASSOCIATED CONTENT

● Supporting Information

NMR spectra of new compounds, thermal ellipsoid plot of the X-ray diffraction structure of **5**, and tables of total energies and atom coordinates from the theoretical calculations. This material is available free of charge via the Internet at <http://pubs.acs.org>.

■ AUTHOR INFORMATION

Corresponding Author

*Fax: + 49 221 470 3083. Tel: + 49 221 470 5057. E-mail: griesbeck@uni-koeln.de.

Notes

The authors declare no competing financial interest.

■ ACKNOWLEDGMENTS

We thank the Deutsche Forschungsgemeinschaft (DFG) (Project Gr-881-13/1) for financial support.

■ REFERENCES

- (1) (a) Alberti, M. N.; Orfanopoulos, M. *Tetrahedron* **2006**, *62*, 10660–10675. (b) Clennan, E. L.; Pace, A. *Tetrahedron* **2005**, *61*, 6605–6691. (c) Clennan, E. L. *Tetrahedron* **2000**, *56*, 9151–9179. (d) Stratakis, M.; Orfanopoulos, M. *Tetrahedron* **2000**, *56*, 1595–1615.
- (2) (a) Adam, W.; Braun, M.; Griesbeck, A. G.; Lucchini, V.; Staab, E.; Will, B. *J. Am. Chem. Soc.* **1989**, *111*, 203–212. (b) Adam, W.; Nestler, B. *J. Am. Chem. Soc.* **1993**, *115*, 7226–7231.
- (3) (a) Alberti, M. N.; Orfanopoulos, M. *Chem.—Eur. J.* **2010**, *16*, 9414–9421. (b) Stephenson, L. M.; Grdina, M. J.; Orfanopoulos, M. *Acc. Chem. Res.* **1980**, *13*, 419–425.
- (4) Maranzana, A.; Ghigo, G.; Tonachini, G. *Chem.—Eur. J.* **2003**, *9*, 2616–2626.
- (5) Orfanopoulos, M.; Stephenson, L. M. *J. Am. Chem. Soc.* **1980**, *102*, 1417–1418.
- (6) Hurst, J. R.; Wilson, S. L.; Schuster, G. B. *Tetrahedron* **1985**, *41*, 2191–2197.
- (7) Singleton, D. A.; Hang, C.; Szymanski, M. J.; Meyer, M. P.; Leach, A. G.; Kuwata, K. T.; Chen, J. S.; Greer, A.; Foote, C. S.; Houk, K. N. *J. Am. Chem. Soc.* **2003**, *125*, 1319–1328.
- (8) Leach, A. G.; Houk, K. N.; Foote, C. S. *J. Org. Chem.* **2008**, *73*, 8511–8519.
- (9) Rehbein, J.; Carpenter, B. K. *Phys. Chem. Chem. Phys.* **2011**, *13*, 20906–20922.
- (10) Griesbeck, A. G.; Goldfuss, B.; Leven, M.; de Kiff, A. *Tetrahedron Lett.* **2013**, *54*, 2938–2941.
- (11) Schweitzer, C.; Schmidt, R. *Chem. Rev.* **2003**, *103*, 1685–1757.
- (12) Di Mascio, P.; Devasagayam, T. P. A.; Kaiser, S.; Sies, H. *Biochem. Soc. Trans.* **1990**, *18*, 1054–1056.
- (13) Bosio, G. N.; Breitenbach, T.; Parisi, J.; Reigosa, M.; Blaikie, F. H.; Pedersen, B. W.; Silva, E. F. F.; Mártire, D. O.; Ogilby, P. R. *J. Am. Chem. Soc.* **2013**, *135*, 272–279.
- (14) Speranza, G.; Manitto, P.; Monti, D. *J. Photochem. Photobiol., B* **1990**, *8*, 51–61.
- (15) Manitto, P.; Speranza, G.; Monti, D.; Gramatica, P. *Tetrahedron Lett.* **1987**, *28*, 4221–4224.
- (16) Wilkinson, F.; Helman, W. P.; Ross, A. B. *J. Phys. Chem. Ref. Data* **1995**, *24*, 663–1021.
- (17) Adam, W.; Krebs, O.; Orfanopoulos, M.; Stratakis, M. *J. Org. Chem.* **2002**, *67*, 8395–8399.
- (18) Griesbeck, A. G.; Adam, W.; Bartoschek, A.; El-Idreesy, T. T. *Photochem. Photobiol. Sci.* **2003**, *2*, 877–881.
- (19) (a) Li, X.; Ramamurthy, V. *J. Am. Chem. Soc.* **1996**, *118*, 10666–10667. (b) Robbins, R. J.; Ramamurthy, V. *Chem. Commun.* **1997**, 1071–1072. (c) Stratakis, M.; Froudakis, G. *Org. Lett.* **2000**, *2*, 1369–1372.
- (20) (a) Griesbeck, A. G.; Cho, M. *Tetrahedron Lett.* **2009**, *50*, 121–123. (b) Griesbeck, A. G.; Uhlig, J.; Sottmann, T.; Belkoura, L.; Strey, R. *Chem.—Eur. J.* **2012**, *18*, 16161–16165.
- (21) (a) Adam, W.; Griesbeck, A. G. *Synthesis* **1986**, 1050–1052. (b) Orfanopoulos, M.; Foote, C. S. *Tetrahedron Lett.* **1985**, *26*, 5991–5994.
- (22) Stensaas, K. L.; Bajaj, A.; Al-Turk, A. *Tetrahedron Lett.* **2005**, *46*, 715–718.
- (23) Gollnick, K.; Griesbeck, A. G. *Tetrahedron* **1984**, *40*, 3235–3250.
- (24) Crystal structure of endoperoxide **5**: deposition number CCDC 945446; C₉H₁₄O₄; a = 6.0161(4) Å, b = 14.424(2) Å, c = 21.643(3) Å; space group *Pbca*.
- (25) Griesbeck, A. G.; de Kiff, A. *Org. Lett.* **2013**, *15*, 2073–2075.

- (26) Yunus, K.; Balci, M. *Tetrahedron* **2003**, *59*, 2063–2066.
- (27) Adam, W.; Richter, M. J. *Acc. Chem. Res.* **1994**, *27*, 57–62.
- (28) Staroverov, V. N.; Scuseria, G. E.; Tao, J. M.; Perdew, J. P. *J. Chem. Phys.* **2003**, *119*, 12129–12137.
- (29) Schäfer, A.; Horn, H.; Ahlrichs, R. *J. Chem. Phys.* **1992**, *97*, 2571–2577.
- (30) Maranzana, A.; Canepa, C.; Ghigo, G.; Tonachini, G. *Eur. J. Org. Chem.* **2005**, 3643–3649.
- (31) Ahlrichs, R.; Bär, M.; Häser, M.; Horn, H.; Kölmel, C. *Chem. Phys. Lett.* **1989**, *162*, 165–169.
- (32) Yadav, J. S.; Pratap, T. V.; Rajender, V. *J. Org. Chem.* **2007**, *72*, 5882–5885.
- (33) Loh, T. G.; Cao, G. Q.; Pei, J. *Tetrahedron Lett.* **1998**, *39*, 1457–1460.
- (34) Ni, Y.; Montgomery, J. J. *Am. Chem. Soc.* **2006**, *128*, 2609–2614.
- (35) Piers, E.; Jung, G. L.; Ruediger, E. H. *Can. J. Chem.* **1987**, *65*, 670–682.
- (36) Kemper, J.; Studer, A. *Angew. Chem., Int. Ed.* **2005**, *44*, 4914–4917.
- (37) Ahmed, M. M.; Mortensen, M. S.; O'Doherty, G. A. *J. Org. Chem.* **2006**, *71*, 7741–7746.
- (38) Moses, J. E.; Baldwin, J. E.; Brückner, S.; Eade, S. J.; Adlington, R. M. *Org. Biomol. Chem.* **2003**, *1*, 3670–3684.
- (39) Lebel, H.; Guay, D.; Paquet, V.; Huard, K. *Org. Lett.* **2004**, *6*, 3047–3050.
- (40) Uriac, P.; Bonnic, J.; Huet, J. *Tetrahedron* **1985**, *41*, 5051–5060.